

Subsurface stratigraphy and micropaleontology of the Neogene rocks, Nile Delta, Egypt



Ahmed A. Ismail, Mohamed Boukhary and Ahmed I. Abdel Naby

Department of Geology, Faculty of Science, Ain Shams University, Abassia 11566, Cairo, Egypt;
(aaaismail2002@yahoo.com; moboukhary@yahoo.com and zowail2000@yahoo.com)

doi: 104154/gc.2010.01

Geologia Croatica

ABSTRACT

Three wells (Naf-2, Naf-3 and Naf-101), were described and sampled in order to increase understanding of the stratigraphy and micropaleontology of the North Abu Qir Field, Nile Delta, Egypt. Lithostratigraphic studies aided recognition of the following Miocene-Pliocene rock formations (from base to top); Qantara Formation, Sidi Salim Formation, Qawasim Formation, Rosetta Formation, Abu Madi Formation, Kafr El Sheikh Formation, Baltim Formation, Mit Ghamr Formation, and Bilqas Formation. Biostratigraphic studies were based on the distribution of foraminifera through the Miocene-Pliocene succession. The environmental conditions of the Neogene rocks of the studied wells are interpreted using the results of palaeoecological parameters (e.g. the total number of foraminifera (T.N.F) and planktonic/benthonic ratio (P/B).

Keywords: Stratigraphy, Neogene, foraminifera, North Abu Qir area, Nile Delta, Egypt

1. INTRODUCTION

The Nile Delta is one of the most well known deltas of the world, and has attracted the attention of many geologists due to its potential gas reserves. The considerable rise of oil and gas prices has led to further exploration in order to locate new hydrocarbon fields. The Nile Delta has in general, a featureless surface with a northward slope, except for some limited topographic features such as the Khatatba positive structural and topographic features, and the westward Wadi El-Natron negative element. Generally, no outcrops occur on the Delta surface, being mainly covered with recent mud and alluvial deposits (AZZAM, 1994), and also with some sand accumulations known as the Turtle-backs.

The structural setting of the Nile Delta region occupies a key position within the plate tectonic development of the eastern Mediterranean and the Levant. It lies on the northern margin of the African Plate, which extends from the subduc-

tion zone adjacent to the Cretan and Cyprus arcs, to the Red Sea where it drifted apart from the Arabian plate. The Abu Qir Field consists of two culminations western and eastern. The western culmination is a four-way dip closure and the eastern culmination is a three-way dip closure and sealed from the eastern direction (cross-fault sealing) by the Kafr El Sheikh Shales, which were brought in juxtaposition with the Abu Madi Sands on the upthrown side of the fault. To the southeast, the West Abu Qir structure is separated from the Abu Qir Gas Field by a northeast-southwest narrow complex graben. This graben was formed by a northeast-southwest trending group of faults (BADRAN, 1996). Structurally, the Abu Qir and West Abu Qir fields were possibly formed in the same way, each being a rollover feature resulting from the slumping of post-Miocene deltaic sediments within the giant graben, which was bounded by almost two east-west major growth faults (BADRAN, 1996).

2. GEOLOGIC SETTING

The Miocene rocks in the Nile Delta region were subdivided by E.G.P.C., (1994) into three formations, from base to top: the Sidi Salim, Qawasim and Rosetta. The Sidi Salem Formation is mainly composed of green-grey clays with a few interbeds of dolomitic marls, and rare occurrences of quartzose sandstones with calcareous cement and siltstones (BARAKAT, 1982). The age of this formation ranges from Langhian to Tortonian. The lower limit is not known in the central part of the Delta, but was encountered in the western offshore area (Abu Qir) E.G.P.C. (1994) and also in the south and southeast. It probably overlies the Moghra Formation or older rocks (BARAKAT, 1982). The type section of this formation is represented by the bottom sequence at the Sidi Salim well 1 (located south of Lake Burullus), from 3592 to 4038 m depth. The upper limit is defined by the base of the thick conglomeratic series of the Qawasim Formation. Offshore the Sidi Salim is overlain directly either by the Rosetta Anhydrite or by the Lower Pliocene clays of the Kafr El Sheikh Formation. Extensive facies changes, both lateral and up-dip, occur within the Sidi Salim Formation in particular, and in Miocene sequence in general (E.G.P.C., 1994).

The Qawasim Formation overlies the Sidi Salem Formation, and underlies the Rosetta Formation. It is composed of a thick, sandy, and conglomeratic sequence, containing a typical rare Messinian fauna of the Mediterranean basin (E.G.P.C., 1994). The sequence is present in the interval from 2800 to 3733 m in the Qawasim 1 well, located some 14 km east of the Sidi Salim well 1 (SCHLUMBERGER, 1984). The upper boundary of this formation is rather difficult to determine if the anhydrites of Rosetta Formation are absent. Locally, it passes laterally to marine clays with Pliocene fauna of Kafr El Sheikh Formation. When the Qawasim Formation occurs within the basal sands of Abu Madi Formation, where the Rosetta Anhydrite is missing, the criteria of separation are based on palaeontological and sedimentological evidence (BARAKAT, 1982).

Large layers of anhydrite, interbedded with thin clays, represent the Rosetta Formation, observed in offshore well Rosetta 2, NE of the mouth of the Rosetta Nile branch, between 678 to 2718 m depth. The presence of the Rosetta Anhydrite seems to be limited only to the northern and offshore part of the Delta. It has not been encountered in wells drilled on the west flank of the Delta (Abu Qir), but was again present offshore to the north of Alexandria. A Messinian age has been attributed to the Rosetta Anhydrite because of its position below the marine shales of definite Early Pliocene age. The formation indicates a general starvation of the sea that affected the whole Mediterranean area and led to the deposition of evaporites SCHLUMBERGER (1984) and HSU et al. (1973, 1977).

The Pliocene rocks in the Nile Delta region are subdivided by E.G.P.C., (1994) into three formations, from base to top: Abu Madi, Kafr El Sheikh, El Wastani. The Abu Madi Formation is represented by a thick series of sands, in part pebbly, with interbedded thin shales. The formation is cross-bedded and overlies the Rosetta Anhydrite, and/or the Qa-

wasim Formation, with a marked unconformity. It is a marine deposit of Early Pliocene age. The shale content increases upward and the contact with the overlying Kafr El Sheikh Formation is gradational in the studied wells. The type section is present in the Abu Madi well 1, between 3007 to 3229 m depth. The Abu Madi Formation is the gas-producing horizon of the Nile Delta (E.G.P.C., 1994).

The Kafr El Sheikh Formation is composed of soft clays with a few interbeds of poorly consolidated sands with a clayey matrix. The development of this series appears to be rather constant over the entire Delta area. Its upper boundary is marked by the first appearance of the El-Wastani sands which have a typical littoral fauna. The Kafr El Sheikh is dated as Early to Middle Pliocene age, according to palaeontological evidence (BARAKAT, 1982). The section has been penetrated in the Kafr El Sheikh well, located some 40 km SSW of the Abu Madi gas field, in the south-central part of the onshore delta area. Its thickness is 1458 m (ISMAIL, 1984).

The El Wastani Formation consists of thick quartzose sandstone interbedded with thin clays which thin towards the top. The upper boundary of this formation is uncertain, but it is delineated where the series becomes more sandy for several tens of metres. This formation is assigned to the Late Pliocene (BARAKAT, 1982), and is 123 m thick in the El Wastani well 1 (ISMAIL, 1984).

Pleistocene–Holocene rocks are subdivided by (E.G.P.C., 1994) into two formations; the Mit Ghamr Formation at the base, and the Bilqas Formation at the top. The Mit Ghamr Formation is composed of thick layers of sands and pebbles at its base with clay interbeds. This formation grades into the overlying Bilqas Formation by the increase of interbedded clays with sands, rich in peat, and fossiliferous, with a coastal or lagoonal fauna. The Bilqas Formation constitutes the top basin fill with coastal sands and deposits from the Nile floods. It was encountered between 20 and 484 m in the Mit Ghamr well, located in the southern part of the Delta, on the east side of the Damietta branch (SCHLUMBERGER, 1984). The Holocene rocks are represented by the intermittent marine transgressions that give rise to a few metres of marine sediments. Both constitute the Bilqas Formation. Plant remains and peat deposits are frequent (E.G.P.C., 1994).

3. MATERIAL AND METHODS

The Abu Qir North Field, Nile Delta, Egypt, is located to the north west of the Rosetta branch of the Nile River, and is bounded between latitudes 31° 34' N & 31° 52' N and longitudes 30° 04' E & 30° 26' E (Fig. 1). The number and depth of ditch cutting samples (in metres) for each well are given in Table 1 below.

Table 1: Location and number of samples taken from each well in the study area.

| Wells | Depth Interval (m) | Number of samples |
|---------|--------------------|-------------------|
| Naf-2 | 1870–3445 | 17 |
| Naf-3 | 1030–3300 | 30 |
| Naf-101 | 1540–3550 | 24 |

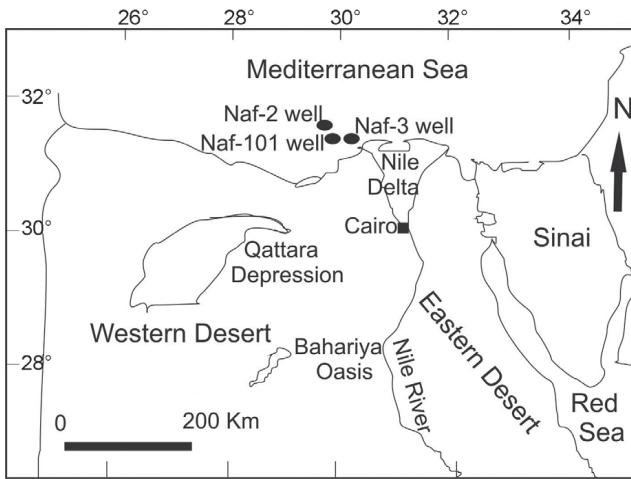


Figure 1: A location map showing the studied wells.

These samples were washed, picked, and the different species of foraminifera have been identified and examined. The aim of this study is to analyze the encountered successions stratigraphically, in order to decipher the depositional environment, depositional processes and lateral and vertical facies changes. To achieve these objectives, the following steps were followed:

1. Identifying and recognizing the different rock units of the penetrated Miocene–Pliocene sequence based on the description of the ditch cutting samples and composite logs.

| Age | Formation | Lithology | Description |
|----------|------------------------|----------------|---|
| Holocene | Bilqas | | Sands and clay interbeds |
| Pliocene | Pleistocene | Mit Ghamr | Clay, sand and silt intercalations with limestone streaks |
| | | | |
| | El Wastani | | |
| | Piacenzian | Kafr El Sheikh | Shale-clay intercalations with some streaks of sands, siltstones, argillaceous limestones and dolomites |
| | Zanclean | | |
| Miocene | Messinian | Abu Madi | Conglomeratic sands with clay interbeds |
| | | Rosetta | Anhydrite with sand and clay streaks |
| | Tortonian-Serravallian | Qawasim | Sands and conglomeratic sandstones with clay interbeds |
| | | Sidi Salem | Shale, sand and clay intercalations with limestone streaks |
| | Langhian-Burdigalian | Marmarica | Reefal limestone |
| | | Moghra | Sandstones, clay and shales |
| | Oligocene | Dabaa | Sandy shales |

Figure 2: The Generalized subsurface stratigraphic column of the Nile Delta region.

2. Identifying the foraminifera obtained from the different horizons and the distribution of the foraminiferal assemblages, for biostratigraphic studies of the Neogene sequence.

3. Delineation of palaeo-sedimentary environments, and the number of depositional cycles by using several palaeoecological parameters (e.g. the total number of foraminifera, (T.N.F.) and planktonic/benthic ratio (P/B).

4. STRATIGRAPHY

Correlation of the three wells located in the North Abu Qir Field revealed ten lithostratigraphic formations (based on lithological characteristics). These are, from base to top, as follows: Qantara Formation, Sidi Salim Formation, Qawasim Formation, Rosetta Formation, Abu Madi Formation, Kafr El Sheikh Formation, El Wastani Formation, Baltim Formation, Mit Ghamr Formation, and Bilqas Formation. Each rock unit is discussed below, taking into consideration the lithologic characters, stratigraphic limits, thickness, and the foraminiferal content when present.

4.1. Qantara Formation

The top of the Qantara Formation is only reached by the Naf-101 well (Figs. 3, 4 and 5), which did not reach the base of this formation. The formation is unconformably overlain by the Sidi Salim Formation. Southward, in the study area, this formation is composed of shale with argillaceous sand and limestone, as revealed by the drilling data in other wells. Northward, the limestone of this formation decreases, and was replaced by clastics (shale and sand). Furthermore, this formation is dated as Early Miocene in age, according to the presence of *Globigerinoides primordius* as shown in (Fig. 6). This age assignment is confirmed by the presence of the Early Miocene *Dentoglobigerina altispira altispira* and *Globorotalia*

| Age | Formation | Lithology | Description |
|-----------------------|--------------------|-----------|---|
| Pleistocene to Recent | Bilqas & Mit Ghamr | | Silty clay interbeds with fine to medium sand, locally lignitic and sandy limestone |
| Pleistocene | Baltim | | Clay with sand and argillaceous limestone interbeds, locally lignitic and silty. Traces of fossil remains |
| Late Pliocene | El Wastani | | Clay with fine to very fine sand and streaks of limestone and dolomite |
| Middle Pliocene | Kafr El Sheikh | | Shale with thin streaks of sands and argillaceous limestones and dolomite. Traces of fossil remains |
| Early Pliocene | | | |
| Late Miocene | Abu Madi | | Shale with sands interbeds |
| | Rosetta | | Anhydrite |
| | Qawasim | | Sands and shale intercalations |
| | Sidi Salem | | Shale |

Figure 3: The stratigraphic column of Naf-2 well.

| Age | Formation | Lithology | Description |
|-----------------------|--------------------|-----------|---|
| Pleistocene to Recent | Bilqas & Mit Ghamr | | Clay with streaks of siltstone Limestone to sandy limestone Intercalations of shale and siltstone |
| | Baltim | | Intercalations of sand, shale, clay and siltstone with rare streaks of limestone |
| Pliocene | El Wastani | | Calcareous and silty clay |
| | Kafr El Sheikh | | Intercalations of sand, shale, clay and siltstone with rare streaks of white limestone |
| | Abu Madi | | Shale with sands intercalations Clay and sandy anhydrite Sands |
| Late Miocene | Rosetta Qawasim | | Intercalations of sand, shale, clay and siltstone with rare streaks of white limestone |
| Early Middle Miocene | Sidi Salem | | Intercalations of sand, shale, clay and siltstone with rare streaks of white limestone |

Figure 4: The stratigraphic column of Naf-3 well.

| Age | Formation | Lithology | Description |
|-----------------------|--------------------|-----------|---|
| Pleistocene to Recent | Bilqas | | Intercalations of sand and shale |
| | Mit Ghamr | | Interbedding of clay and sand, with lignite and limestone remains |
| Pleistocene | Baltim | | Interbedding of sand, shale, clay and limestone with lignite traces |
| Pliocene | El Wastani | | Interbedding of sand, shale, clay with lignite traces |
| | Kafr El Sheikh | | Intercalations of sand, shale, clay and siltstone with rare streaks of white limestone and dolomite |
| | Abu Madi | | Interbedding of shale, sands and clay |
| Late Miocene | Rosetta Qawasim | | Anhydrite Sand and clay |
| Middle Miocene | Sidi Salem | | Intercalations of sand, shale, clay and siltstone with rare streaks of white limestone |
| Early Miocene | Qantara | | Interbedding of calc. shale, sands and clay |

Figure 5: The stratigraphic column of Naf-101 well.

obesa. Also, there are several other planktonic species associated with these fossils (e.g. *Globigerinoides bisphericus*, *Neogloboquadrina continuosa*, *Globorotalia archeomerandii*, *Globigerina brazieri*, *Globigerina praebulloides*, *Orbulina cf. suturalis*, *Orbulina universa* and *Globigerinoides trilobus immaturus*). Moreover, there are several benthic species associated with the previous planktonic species e.g. (*Bolivina dilatata*, *Gyroidinoides soldanii*, *Nonionina scapha*, *Bulimina elongata*, *Lagena sulcata*, *Globocassidulina elongata*, *Uvigerina semiornata*, *Nonionella auris*, *Lenticulina cultrata*, *Cibicides refulgens* and *Neoeponides* sp).

| Age | Planktonic foraminiferal zones and subzones | | |
|----------|---|---|--|
| Pliocene | L | <i>Globorotalia tosaensis tosaensis</i> | |
| | M | <i>Globorotalia miocenica</i> <i>Gr. exilis</i> <i>Gr. trilob.fistulosus</i> | |
| | | <i>Globorotalia margaritae</i> <i>Globorotalia marg. evoluta</i> <i>Globorotalia marg. margaritae</i> | |
| Miocene | L | <i>Globorotalia humerosa</i> <i>Globorotalia acostaensis</i> | |
| | | M | <i>Globorotalia menardii</i> <i>Globorotalia mayeri</i> <i>Globigerinoides ruber</i> <i>Globorotalia fohsi robusta</i> <i>Globorotalia fohsi lobata</i> <i>Globorotalia fohsi fohsi</i> |
| | E | | <i>Globorotalia fohsi</i> <i>Præorbulina glomerosa</i> <i>Globigerinella insueta</i> <i>Catapsydrax stainforthi</i> <i>Catapsydrax dissimilis</i> <i>Globigerinoides primordius</i> |

Figure 6: The Miocene–Pliocene planktonic foraminifera zones and subzones (after BOLLI & SAUNDERS, 1985). E – Early, M – Middle, L – Late.

4.2. Sidi Salim Formation

This formation unconformably overlies the Qantara Formation and underlies the Qawasim Formation. The bottom of this formation was not reached in two wells (Naf-2 and Naf-3). Its thickness in well Naf-101 is 460 m. This formation is composed of intercalations of shale, sand, clay, with rare occurrences of white, bioclastic limestone. This limestone occurs less frequently and passes gradually towards the north-east of the study area. The formation is of Middle Miocene age, based on the presence of *Globigerinoides bollii* at the top of this formation, which could represent a useful datum in the Mediterranean region, where the *Globigerinoides fohsi* lineage is not developed (BOLLI & SAUNDERS, 1985). However, the absence of the three upper biozones of Middle Miocene age (*Globigerinoides ruber*, *Neogloboquadrina mayeri* and *Globorotalia menardii*) biozones indicates a hiatus between the Middle Miocene and the Late Miocene as shown on the distribution chart of the Naf-101 well (Fig. 12). However, the presence of *Præorbulina glomerosa curva* and *Præorbulina glomerosa glomerosa* species supports the age assignment of this formation, which directly underlies the Upper Miocene sediments. This also indicates a similar hiatus in the formation as shown in the Naf-3 well (Fig. 11). Accordingly, this formation is dated from the Early Middle Miocene to Late Miocene.

Also, there are several planktonic species associated with the above species (e.g. *Globigerinoides pseudobesa*, *Globigerina ciperoensis ciperoensis*, *Dentoglobigerina venezuelana*, *Globigerina woodi*, *Globigerina nilotica*, *Orbulina universa*, *Orbulina bilobata*, *Globigerinoides trilobus immaturus*, *Globigerinoides obliquus extremus* and *Globigerinella obesa*). Moreover, there are several benthic species associated with the planktonic taxa listed above (e.g. *Quinqueloculina boschiana*, *Bolivina hebes*, *Ammonia beccarii*, *Bulimina elongata*, *Asterigerina planorbis*, *Nonionellina cf. labradorica*, *Gyroidinoides soldanii*, *Pullenia quinqueloba*, *Elphidium macellum* and *Neoponides* sp.).

4.3. Qawasim Formation

This formation overlies the Sidi Salim Formation and underlies the Rosetta Formation. The thickness of this formation increases northward (25 m in the Naf-101 well, and 100.5 m in the Naf-2 well (Fig. 3)). Also, its thickness is 34 m in Naf-3 well. This formation is composed of sand to sandstone with a few interbeds of clay. Also, there are several planktonic species associated with this formation (e.g. *Globigerinoides trilobus immaturus*, *Globigerinoides bullatus*, *Globigerinoides obliquus extremus*, *Globigerina nilotica*, and *Orbulina universa*). Moreover, there are several benthic species associated with the planktonics (e.g. *Cibicides gibbosus*, *Alabamina* sp., *Buccella* sp., *Uvigerina cf. asperula*, *Bolivina hebes*, and *Nonionina scapha*). The formation has been dated as Late Miocene (Messinian), according to its stratigraphic position (AZZAM, 1990; E.G.P.C., 1994; and ABU EL ENEIN, 1990) and also on both lithological and palaeontological characteristics (ISMAL, 1984). In the present study, this formation is also dated as Late Miocene according to its stratigraphic position between the underlying Sidi Salim Formation of Early Middle Miocene to Late Miocene and the overlying Rosetta Formation of Late Miocene.

4.4. Rosetta Formation

This formation overlies the Qawasim Formation and underlies the Abu Madi Formation. The thickness of this formation decreases northward (99 m in Naf-101 well and 28 m in Naf-2 well). Also, its thickness is 50 m in Naf-3 well. It is composed of sand with occurrences of anhydrite and clay. Deposition of evaporites in this formation indicates a general regression of the Mediterranean, and this also explains the low content of planktonic foraminiferal species (e.g. *Globigerinoides tenellus*, *Globigerinoides obliquus extremus*, *Globigerina nilotica*, *Orbulina bilobata* and *Orbulina universa*). Also, there are few benthic species associated with the planktonics (e.g. *Gyroidinoides soldanii*, *Alabamina* sp., *Uvigerina semiornata* and *Loxostomum pseudodigitale*). The age of the Rosetta Formation is Late Miocene (Messinian) due to its stratigraphic position below the Upper Miocene–Lower Pliocene marine sediments (Abu Madi Formation). Also, the presence of *Sphaeroidinellopsis disjuncta* in the topmost part of this formation is further evidence for this age assignment. This species of *Sphaeroidinellopsis* has been used repeatedly as a zonal marker (BOLLI & SAUNDERS,

1985). The highest occurrence of *Sphaeroidinellopsis disjuncta* denotes the top of the Miocene (BOLLI & SAUNDERS, 1985).

4.5. Abu Madi Formation

This formation overlies the Rosetta Formation and/or the Sidi Salim Formation with a marked unconformity and underlies the Kafr El Sheikh Formation. The thickness of this formation increases northward (138 m in Naf-101 well and 234 m in Naf-2 well). Also, its thickness attains 155 m in Naf-3 well (Fig. 4). It is mainly composed of intercalations of sand, clay, and shale. The age assignment of this formation is controversial, where it is dated as Late Miocene (Messinian), on a sedimentological basis, by EFFAT & GEZEIRY (1986) and DEIBIS et al. (1986). However, ABU EL ENEIN (1990) stated that the transgression in the Early Pliocene was responsible for deposition of the Abu Madi Formation. In the present study, this formation is dated as Early Pliocene in the studied three wells, according to the presence of *Globorotalia margaritae*, which is a widely recognized index species for the Pliocene (BOLLI & SAUNDERS, 1985). On palaeomagnetic evidence (CITA, 1975 and LOURENS et al., 2004), the age of this species ranges from 5.01 to 4.14 Ma. It is a cosmopolitan species occurring in both deep and shallow waters (BOLLI & SAUNDERS, 1985). The presence of *Globorotalia exilis* with *Globorotalia margaritae* terminates the Early Pliocene according to BOLLI & SAUNDERS (1985). The occurrence of *Sphaeroidinellopsis disjuncta* in the top of the Abu Madi Formation in the Naf-2 well suggests that this formation is of Late Miocene age.

This age assignment is confirmed by the occurrence of *Globorotalia margaritae margaritae* at the base of the overlying Kafr El Sheikh Formation. Also, there are several planktonic species associated with the species listed above (e.g. *Globigerinoides quadrilobatus*, *Globigerinoides obliquus extremus*, *Globigerinoides ruber*, *Globigerinoides bulloides*, *Globigerinoides tenellus*, *Globigerinoides trilobus immaturus*, *Globigerina quinqueloba*, *Globigerina nilotica*, *Globigerina apertura*, *Globigerinella obesa*, *Orbulina universa* and *Catapsydrax parvulus*). Moreover, there are several benthic species associated with the planktonic taxa (e.g. *Bolivina dilatata*, *Loxostomum perforatum*, *Buccella* sp., *Nonionina scapha*, *Lenticulina smiley*, *Alabamina* sp., *Cibicides* sp., *Eponides polygonus*, *Asterigerina planorbis* and *Bulimina elongata*). From the previous discussion, this formation could be classified as Late Miocene–Early Pliocene.

4.6. Kafr El Sheikh Formation

This formation overlies the Abu Madi Formation and underlies the El Wastani Formation. The thickness of this formation is 1121 m in the Naf-101 well and 1149 m in the Naf-2 well. Also, its thickness attains 1282 m in the Naf-3 well. The formation is composed of shale-clay intercalations with some minor occurrences of sands, siltstones, argillaceous limestones, and dolomites. Also, there are several planktonic species present in this formation (e.g. *Globigerinoides obliqua*, *Globigerinoides trilobus trilobus*, *Globigerina falcon-*

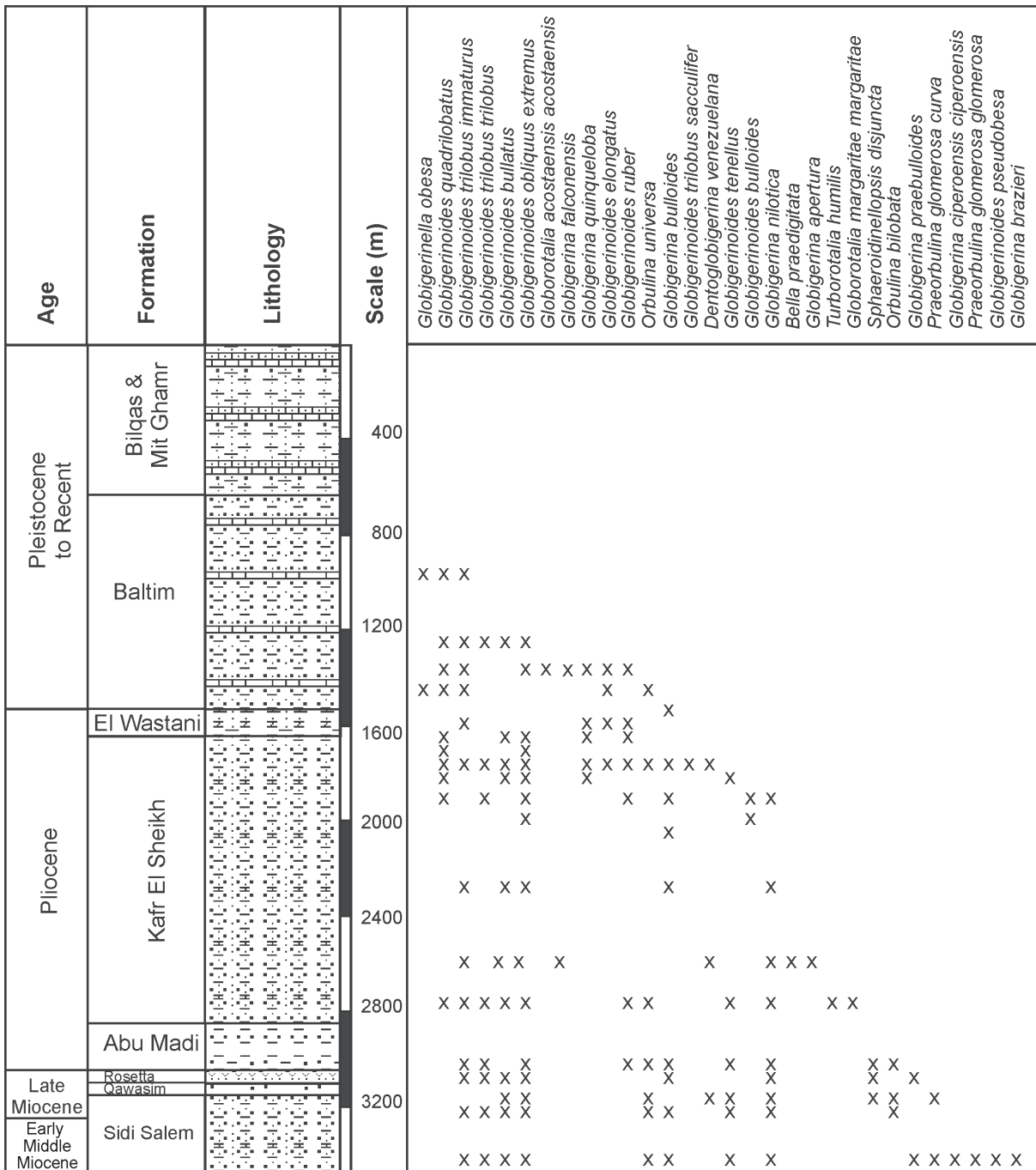


Figure 8: The planktonic foraminiferal distribution chart of Naf-3 well.

ral planktonic species present in this formation (e.g. *Globigerinoides elongatus*, *Globigerinoides trilobus sacculifer*, *Globigerina rubescens*, *Globigerina bulloides*, *Orbulina universa* and *Globigerinella obesa*). There are also several benthic species associated with the planktonic forms (e.g. *Nonion asterizans*, *Ammonia tepida*, *Natlandia cf. secasensis*, *Eponidella cf. libertadensis*, *Lenticulina reedi*, *Bulimina elongata*, *Cassidulina brocha*, *Ammonia umbonata*, *Bolivina hebes* and *Pullenia osloensis*).

The age of this formation is Late Pliocene, based on geophysical data (BADRAN, 1996 and AZZAM, 1994). These authors mentioned that the regression of the sea heralded the end of the sedimentation cycle of the Pliocene.

4.8. Baltim Formation

This formation overlies the El Wastani Formation and underlies the Mit Ghamr Formation. The thickness of this formation is 690 m in Naf-101 well, 986 m in Naf-2 well and 1492 m in the Naf-3 well. The Baltim Formation is composed of intercalations of clay, sand, shale, with thin bioclastic limestones. Planktonic foraminiferal species present in this formation include; *Globigerinella obesa*, *Globigerinoides quadrilobatus*, *Globigerinoides trilobus immaturus*, *Globigerinoides trilobus trilobus*, *Globigerinoides obliquus extremus*, *Globigerinoides ruber*, *Globorotalia acostaensis acostaensis*, *Globigerina falconensis*, *Globigerina quinqueloba* and *Orbulina universa*. There are also several benthic species

as Late Pliocene to Quaternary, while AZZAM (1994) ascribed it to the Pleistocene age. Moreover, BADRAN (1996) dated it as Late Pliocene to Pleistocene in age. In the study area, this formation is dated Pleistocene to Recent throughout, based on correlation with neighbouring areas.

4.10. Bilqas Formation

This formation covers the whole Delta region. In the study area, it is present at the top of all wells. However, it is difficult to differentiate it from the underlying Mit Ghamr For-

mation. This formation is composed of sand interbedded with clay rich in molluscan fragments. The clays contain vegetable remains and carbonaceous matter. It is dated as Holocene by BARAKAT (1982) and BADRAN (1996). AZZAM (1994) mentioned that during the Holocene a marine transgression covered most of the Northern Delta area and gave rise to a few metres of marine sediments capped by agricultural soil. RIZZINI et al. (1976) and ABU EL ENEIN (1990) ascribed this formation to the same age, based on the faunal association. In the study area, this formation is dated as being Pleistocene to Recent in age.

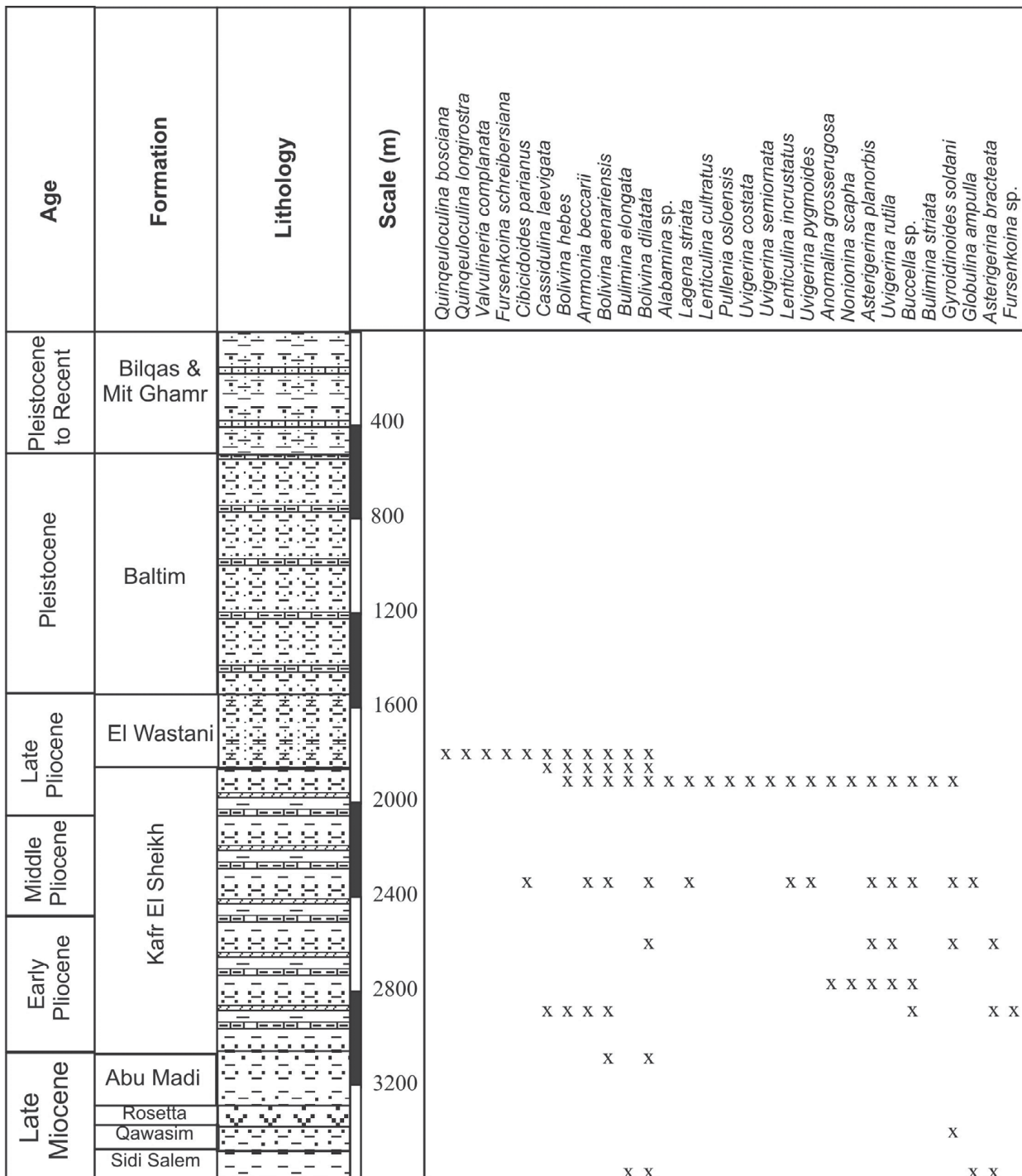
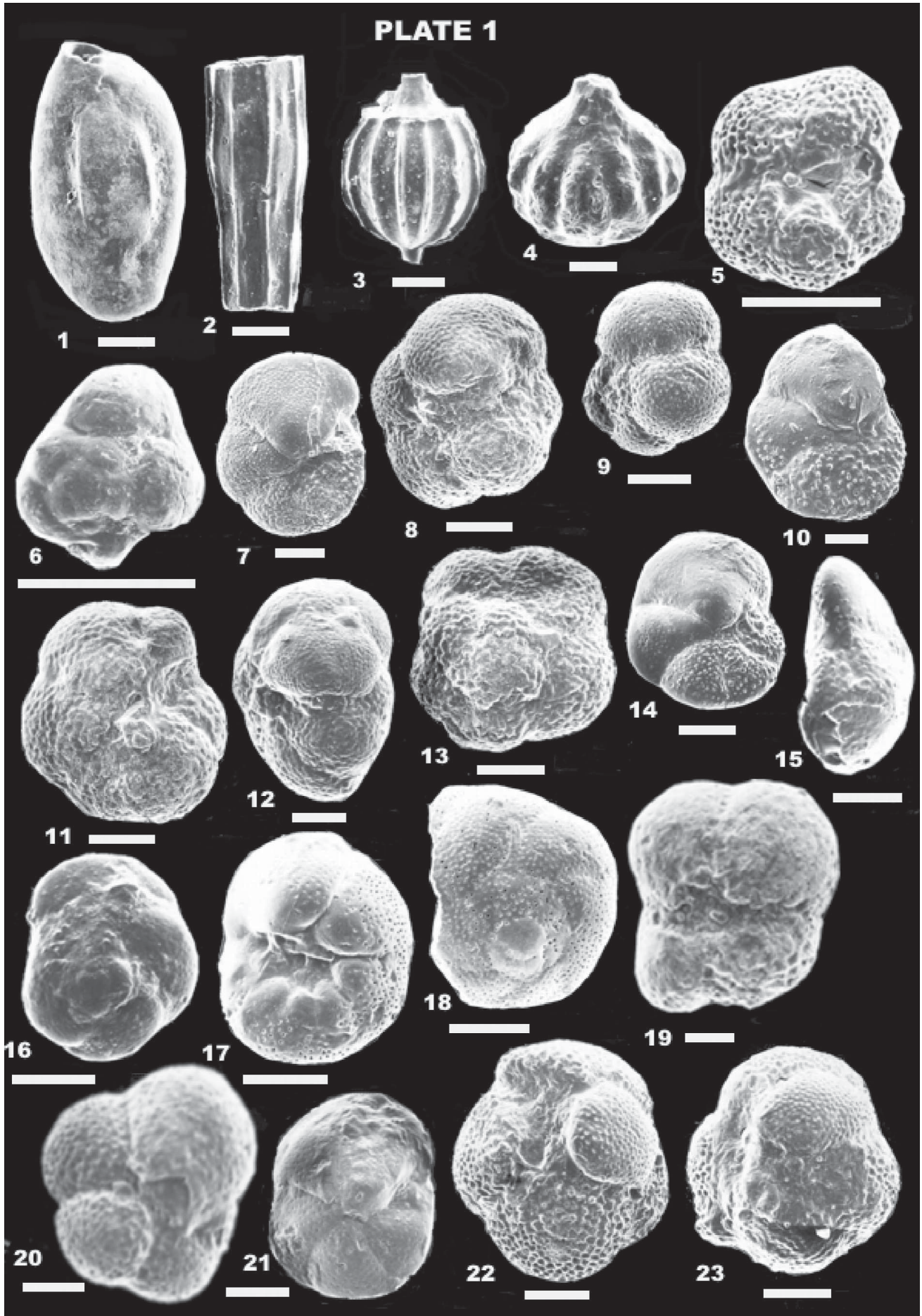


Figure 10: The benthic foraminiferal distribution chart of Naf-2 well.

PLATE 1



***Neogloboquadrina continuosa* (Blow, 1959)**

(Pl. 1, Figs. 8–9)

1959. *Globorotalia opima* Bolli subsp. *continuosa* BLOW, p. 218, pl. 19, figs. 125a–c1985. *Globorotalia continuosa* BLOW-BOLLI et al., p. 204, pl. 28, figs. 8–14.***Globorotalia exilis* BLOW, 1969**

(Pl. 1, Fig. 10)

1969. *Globorotalia cultrata exilis* BLOW, p. 396, pl. 7, figs. 1–3, pl. 42, figs. 1–51983. *Globorotalia exilis*, BLOW-BOLLI et al., p. 228, figs. 33.4, 35.9–11***Globorotalia humerosa humerosa*****TAKAYANAGI & SAITO, 1962**

(Pl. 1, Figs. 11–13)

1962. *Globorotalia humerosa humerosa* TAKAYANAGI & SAITO, p. 78, pl. 28, figs. 1a–c1985. *Globorotalia humerosa humerosa* TAKAYANAGI & SAITO-BOLLI et al, p. 208, figs. 27.8a–c, p. 209, figs. 28.15a–c***Globorotalia margaritae margaritae*****BOLLI & BERMUDEZ, 1965**

(Pl. 1, Figs. 14–16)

1965. *Globorotalia margaritae* BOLLI & BERMUDEZ, p. 132, pl. 1, figs. 16–181985. *Globorotalia margaritae margaritae* BOLLI & BERMUDEZ-BOLLI et al., p. 218, figs. 30.9–14G***Globorotalia peripheroronda* BLOW & BANNER, 1966**

(Pl. 1, Figs. 17–18)

1966. *Globorotalia peripheroronda* BLOW & BANNER, p. 294, pl. 1, figs. 1a–c1983. *Globorotalia peripheroronda* BLOW & BANNER-KENNETT & SRINIVASAN, pl. 22, figs. 1–3***Globorotalia pseudopima* BLOW, 1969**

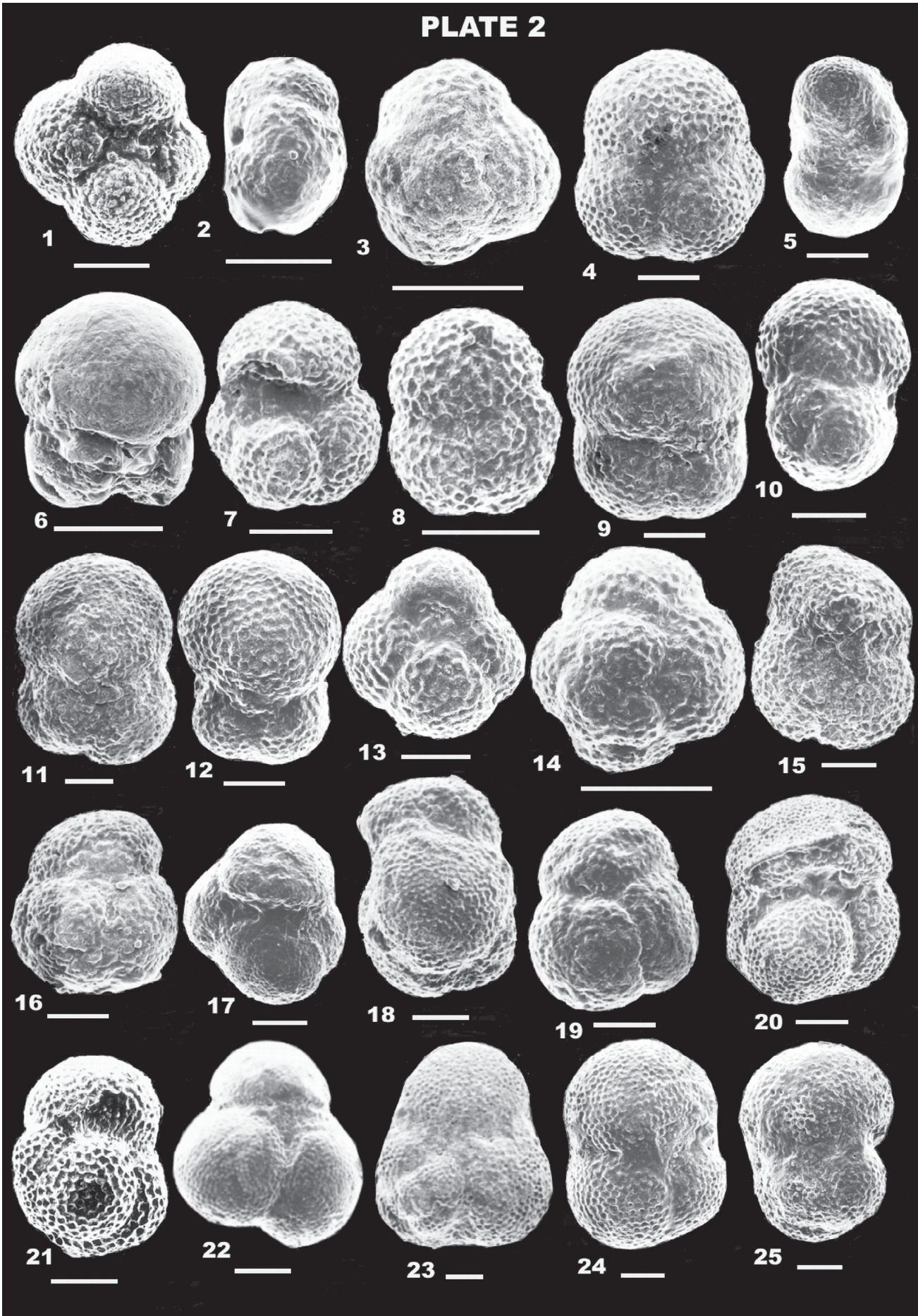
(Pl. 2, Fig. 19)

1969. *Globorotalia acostaensis pseudopima* BLOW, p. 387, pl. 35, figs. 1–31985. *Globorotalia pseudopima* BLOW-BOLLI et al., p. 208, fig. 27.7G, p. 209, figs. 28.10–12G**Plate 1**

Bar scale = 100 µm

- 1 *Quinqueloculina boschiana*, (D'Orbigny 1839), Pleistocene-Recent, Baltim, sample from 1030 m, Naf-3 well.
- 2 *Nodosaria raphanistrum*, Linne 1758, Pleistocene-Recent, Baltim, sample from 1030 m, Naf-3 well.
- 3 *Lagena striata*, (D'Orbigny, 1839), Pliocene, Kafr El Sheikh, sample from 1790 m, Naf-3 well.
- 4 *Lagena sulcata*, (Walker and Jacob, 1798), Early Miocene, Qantara, sample from 3550 m, Naf-101 well.
- 5–6 *Globorotalia acostaensis acostaensis*, Blow 1959,
5. Ventral view, Pleistocene-Recent, Baltim, sample from 1320m, Naf-3 well.
6. Dorsal view, Early Pliocene, Kafr El Sheikh, sample from 3075m, Naf-2 well.
- 7 *Globorotalia archeomenardii*, Bolli 1957, ventral view, Pliocene, Kafr El Sheikh, sample from 2680 m, Naf-101 well.
- 8–9 *Neogloboquadrina continuosa*, Blow 1959,
8. Ventral view, Early Miocene, Qantara, sample from 3530m, Naf-101 well.
9. Dorsal view, Early Miocene, Qantara, sample from 3530m, Naf-101 well.
- 10 *Globorotalia exilis*, Blow 1969, ventral view, Pliocene, Kafr El Sheikh, sample from 2680 m, Naf-101 well.
- 11–13 *Globorotalia humerosa humerosa*, Takayanagi & Saito 1962,
11. Ventral view, Early Miocene, Qantara, sample from 3530m, Naf-101 well.
12. Side view, Early Miocene, Qantara, sample from 3530m, Naf-101 well.
13. Dorsal view, Early Miocene, Qantara, sample from 3530m, Naf-101 well.
- 14–16 *Globorotalia margaritae margaritae*, Bolli & Bermudez 1965,
14. Ventral view, Pliocene, Kafr El Sheikh, sample from 2680 m, Naf-101 well.
15. Side view, Pliocene, Kafr El Sheikh, sample from 3075 m, Naf-2 well.
16. Dorsal view, Pliocene, Abu Madi, sample from 2800 m, Naf-3 well.
- 17–18 *Globorotalia peripheroronda*, Blow & Banner 1966,
17. Ventral view, Pliocene, Kafr El Sheikh, sample from 1980m, Naf-101 well.
18. Dorsal view, Pliocene, Kafr El Sheikh, sample from 19800m, Naf-101 well.
- 19 *Globorotalia pseudopima*, Blow 1969, ventral view, Pliocene, Kafr El Sheikh, sample from 1980 m, Naf-101 well.
- 20 *Globorotalia scitula praescitula*, Blow 1959, ventral view, Early Pliocene, Kafr El Sheikh, sample from 2775 m, Naf-2 well.
- 21 *Globorotalia scitula scitula*, Brady 1884, ventral view, Early Miocene, Qantara, sample from 3530 m, Naf-101 well.
- 22 *Dentoglobigerina altispira altispira*, Cushman & Jarvis 1936, ventral view, Early Miocene, Qantara, sample from 3550 m, Naf-101 well.
- 23 *Globigerina ciperoensis ciperoensis*, Bolli 1954, ventral view, Middle Miocene, Sidi Salim, sample from 3300 m, Naf-3 well.

PLATE 2



***Globorotalia scitula praescitula* BLOW, 1959**

(Pl. 2, Fig. 20)

1957. *Globorotalia scitula praescitula* BLOW, p. 221, pl. 19, figs. 128a–c1985. *Globorotalia scitula praescitula* BLOW-BOLLI et al., p. 219, figs. 31.6a–c***Globorotalia scitula scitula* (BRADY, 1884)**

(Pl. 2, Fig. 21)

1882. *Pulvinulina scitula* BRADY, p. 716.1884. *Globorotalia scitula scitula* BRADY, pl. 103, figs. 7a–c1985. *Globorotalia scitula scitula* BRADY-BOLLI et al., p. 219, figs. 31.3–4G***Dentoglobigerina altispira altispira*, (CUSHMAN & JARVIS 1936)**

(Pl. 2, Fig. 22)

1936. *Globoquadrina altispira* CUSHMAN & JARVIS, p. 5, pl. 1, figs. 13a–c1983. *Globoquadrina altispira altispira* CUSHMAN & JARVIS-BOLLI & SAUNDERS, p. 183, fig. 15***Globigerina ciperoensis ciperoensis* BOLLI, 1957**

(Pl. 2, Fig. 23)

1957. *Globigerina ciperoensis angustiumbilitata* BOLLI, p. 109, pl. 22, figs. 12a–c1985. *Globigerina ciperoensis ciperoensis* BOLLI-BOLLI et al., p. 178, figs. 13.1–3G***Globigerina nilotica* VIOTTI & MANSOUR, 1969 |**

(Pl. 2, Figs. 1–3)

1969. *Globigerina nilotica* VIOTTI & MANSOUR, p. 447, pl. 6, figs. 1–7***Globigerina praebulloides* BLOW, 1959**

(Pl. 2, Fig. 4–6)

1957. *Globigerina praebulloides* BLOW, p. 180, pl. 8 figs. 47a–c; pl. 9, fig. 481983. *Globigerina praebulloides* BLOW-KENNETT & SRINIVASAN, pl. 6, figs. 1–3**Plate 2**

Bar scale = 100 µm

1–3 *Globigerina nilotica*, Viotti & Mansour, 1969,

1. Ventral view, Pliocene, El Wastani, sample from 1540, Naf-101 well.
2. Side view, Late Miocene, Rosetta, sample from 2970, Naf-3 well.
3. Dorsal view, Late Miocene, Rosetta, sample from 2970, Naf-3 well.

4–6 *Globigerina praebulloides*, Blow 1959,

4. Ventral view, Middle Miocene, Sidi Salim, sample from 3300, Naf-3 well.
5. Side view, Mid.-Lat. Miocene, Qawasim, sample from 3300, Naf-3 well.
6. Dorsal view, Middle Miocene, Rosetta, sample from 3030, Naf-101 well.

7–8 *Globigerina rubescens*, Honza, 1980,

7. Ventral view, Late Pliocene, Kafr El Sheikh, sample from 1960 m, Naf-2 well.
8. Dorsal view, Late Pliocene, Kafr El Sheikh, sample from 1960 m, Naf-2 well.

9–12 *Globigerinoides bisphericus*, Todd 1954,

9. Ventral view, Early Miocene, Qantara, sample from 3530 m, Naf-101 well.
10. Dorsal view, Early Miocene, Qantara, sample from 3530 m, Naf-101 well.
11. Side view, Early Miocene, Qantara, sample from 3530 m, Naf-101 well.
12. Side view, Early Miocene, Qantara, sample from 3530 m, Naf-101 well.

13–14 *Globigerinoides bollii*, Blow 1959,

13. Ventral view, Middle Pliocene, Kafr El Sheikh, sample from 2370 m, Naf-2 well.
14. Dorsal view, Late Pliocene, Kafr El Sheikh, sample 1960 m, Naf-2 well.

15–16 *Globigerinoides elongatus*, D'Orbigny 1926,

15. Ventral view, Late Pliocene, Kafr El Sheikh, sample from 1960 m, Naf-2 well.
16. Dorsal view, Late Pliocene, Kafr El Sheikh, sample from 1960 m, Naf-2 well.

17–19 *Globigerinoides obliquus extremus*, Bolli & Bermudez 1965,

17. Ventral view, Late Miocene, Rosetta, sample from 3030, Naf-101 well.
18. Side view, Late Pliocene, Kafr El Sheikh, sample from 1960m, Naf-2 well.
19. Dorsal view, Late Pliocene, Kafr El Sheikh, sample from 1969m, Naf-2 well.

20 *Globigerinoides obliquus obliquus*, Bolli 1957, ventral view, Pliocene, Kafr El Sheikh, sample from 2680 m, Naf-101 well.**21 *Globigerinoides primordius*, Blow & Banner 1962, ventral view, Early Miocene, Qantara, sample from 3550 m, Naf-101 well.****22–23 *Globigerinoides ruber*, D'Orbigny 1839,**

22. Ventral view, Early Pliocene, Kafr El Sheikh, sample from 2625 m, Naf-2 well.
23. Dorsal view, Middle Miocene, Sidi Salim, sample from 3300m, Naf-3 well.

24–25 *Globigerinoides trilobus immaturus*, Le Roy 1939,

24. Ventral view, Middle Miocene, Sidi Salim, sample from 3300m, Naf-3 well.
25. Dorsal view, Middle Miocene, Sidi Salim, sample from 3300 m, Naf-3 well.

***Globigerina rubescens* HOFKER, 1956**

(Pl. 2, Figs. 7–8)

1956. *Globigerina rubescens* HOFKER, p. 234, pl. 32, fig. 26; pl. 35, figs. 18–211983. *Globigerina rubescens* HOFKER-KENNETT & SRINIVASAN, pl. 9, figs. 7–9***Globigerinoides bisphericus* TODD, 1954**

(Pl. 2, Figs. 9–12)

1954. *Globigerinoides bisperica* TODD, p. 681, pl.1, figs. 1a–c1983. *Globigerinoides bisphericus* TODD-BOLLI & SAUNDERS, p. 199, figs. 24.8; 7,9,12***Globigerinoides bollii* BLOW, 1959**

(Pl. 2, Figs. 13–14)

1957. *Globigerinoides bollii* BLOW, p. 189, pl. 10, figs. 65a–c1983. *Globigerinoides bollii* BLOW-BOLLI et al., p. 193, figs. 20.8a–c***Globigerinoides elongatus* (D'ORBIGNY), 1926**

(Pl. 2, Figs. 15–16)

1926. *Globigerina elongata* D'ORBIGNY, p. 277.1985. *Globigerinoides elongatus* (D'ORBIGNY)-BOLLI et al., p. 193, figs. 20.4a–c***Globigerinoides obliquus extremus*****BOLLI & BERMUDEZ, 1965**

(Pl. 2, Figs. 17–19)

1965. *Globigerinoides obliquus extremus* BOLLI & BERMUDEZ, p. 139, pl. 1, figs. 10–121985. *Globigerinoides obliquus extremus* BOLLI & BERMUDEZ-BOLLI & SAUNDERS, p. 194, pl. 20, fig. 11***Globigerinoides obliquus obliquus* BOLLI, 1957**

(Pl. 2, Fig. 20)

1957. *Globigerinoides obliquus* BOLLI, p. 113, pl.25, figs. 19a–c1983. *Globigerinoides obliquus obliquus* BOLLI-BOLLI & SAUNDERS, p. 194, pl. 20, fig. 12***Globigerinoides primordius* BLOW & BANNER, 1962**

(Pl. 2, Fig. 21)

1962. *Globigerinoides primordius* BLOW & BANNER, p. 15, pl. ix, figs. Dd–Ff1983. *Globigerinoides primordius* BLOW & BANNER-KENNETT & SRINIVASAN, pl. 11, figs. 1–3***Globigerinoides ruber* D'ORBIGNY, 1839**

(Pl. 2, Figs. 22–23)

1839. *Globigerinoides ruber* D'ORBIGNY, p. 19, pl. 3, figs. 8a–c1983. *Globigerinoides ruber* D'ORBIGNY-BOLLI et al., p. 193, figs. 20.1, 2***Globigerinoides trilobus immaturus* LE ROY, 1939**

(Pl. 2, Figs. 24–25; Pl. 3, Fig. 1)

1939. *Globigerinoides sacculifer* (Brandy) var. *immaturus* LE ROY, p. 263, pl. 3, figs. 19–211983. *Globigerinoides trilobus immaturus* LEROY-BOLLI et al., p. 193, figs. 20.14a–c***Globigerinoides trilobus sacculifer* BRADY, 1877**

(Pl. 3, Fig. 2)

1877. *Globigerina sacculifera* BRADY, p. 535.1985. *Globigerinoides trilobus sacculifer* BRADY-BOLLI et al., p. 193, figs. 20.13a–b***Globigerinoides trilobus trilobus* (REUSS), 1850**

(Pl. 3, Figs. 3–5)

1850. *Globigerina triloba* REUSS, p. 374, pl. 47, figs. 11a–c1985. *Globigerinoides trilobus trilobus* (REUSS)-BOLLI et al., p. 193, figs. 20.15a–b***Sphaeroidinellopsis disjuncta* FINLAY, 1940**

(Pl. 3, Figs. 6–8)

1939. *Sphaeroidinellopsis disjuncta* FINLAY, p. 467, pl. 67, figs. 224–2281983. *Sphaeroidinellopsis disjuncta* FINLAY-KENNETT & SRINIVASAN, pl. 51, figs. 3–5***Orbulina bilobata* D'ORBIGNY, 1846**

(Pl. 3, Fig. 9)

1846. *Orbulina bilobata* D'ORBIGNY, p. 164, pl. 9, figs. 11–141983. *Orbulina bilobata* D'ORBIGNY, KENNETT & SRINIVASAN, p. 88, pl. 20, figs. 7–9***Orbulina cf. suturalis* BRONNIMANN**

(Pl. 3, Fig. 10)

1951 *Orbulina suturalis* BRONNIMANN, p. 135, figs. 2–41985 *Orbulina suturalis* BRONNIMANN-BOLLI & SAUNDERS, p. 201, fig. 23 (2)***Orbulina universa* D'ORBIGNY, 1839**

(Pl. 3, Fig. 11)

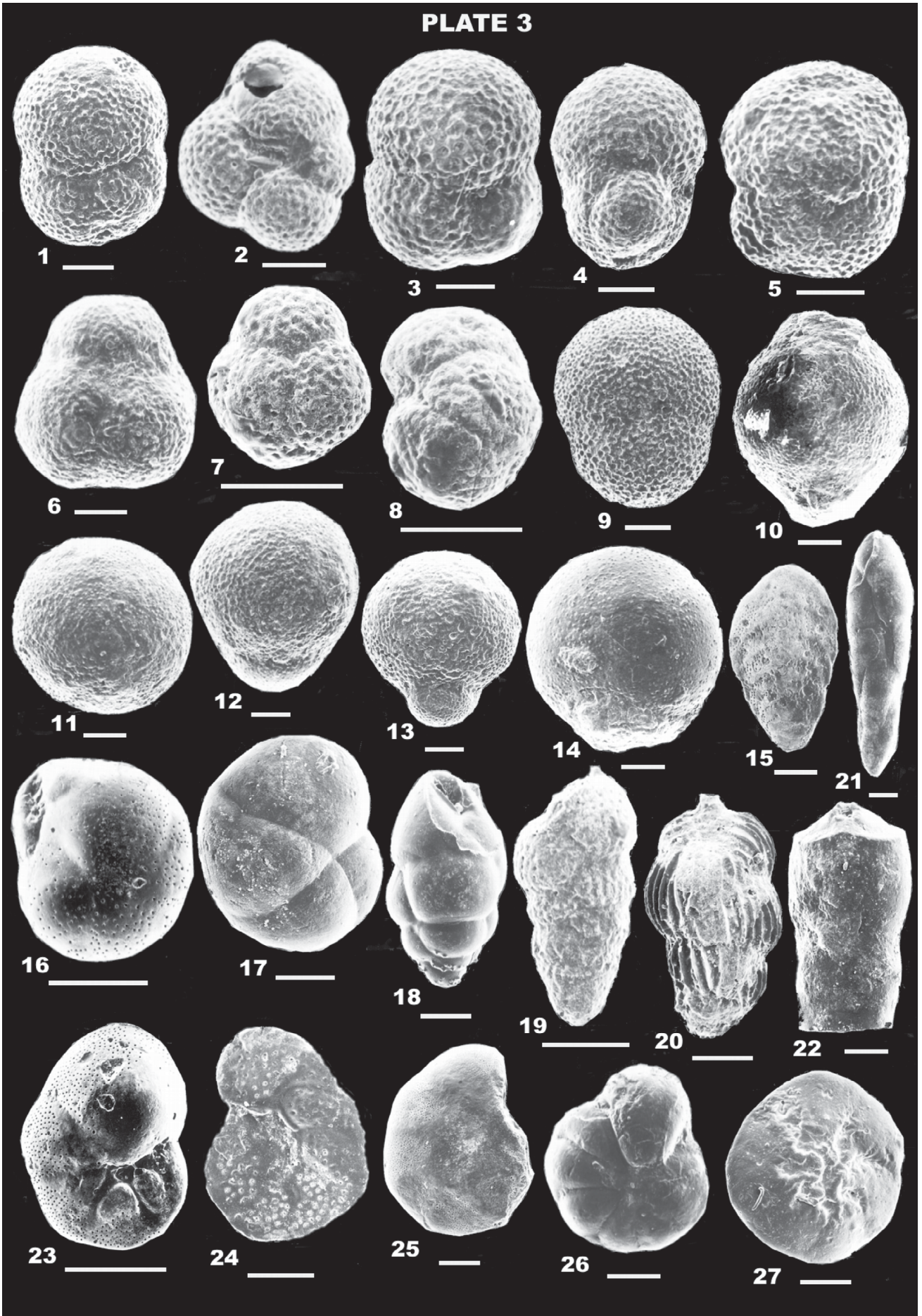
1839. *Orbulina universa* D'ORBIGNY, p. 3, pl. 1, fig. 11983. *Orbulina universa* D'ORBIGNY-KENNETT & SRINIVASAN, pl. 18, fig. 2; pl. 20, figs. 4–6***Praeorbulina glomerosa curva* BLOW, 1956**

(Pl. 3, Figs. 12–13)

1956. *Praeorbulina glomerosa curva* BLOW, p. 62, Text fig. 1, no. 9–14

1983. *Praeorbulina glomerosa curva* BLOW-KENNETT & SRINIVASAN, pl. 18, figs. 3–4
- Praeorbulina glomerosa glomerosa* BLOW, 1956**
(Pl. 3, Figs. 14)
1956. *Praeorbulina glomerosa glomerosa* BLOW, p. 64, Text fig. 1, 15–19. fig. 2, 1–2
1983. *Praeorbulina glomerosa glomerosa* BLOW-KENNETT & SRINIVASAN, pl. 18, figs. 5–7
- Bolivina hebes* MACFADYEN, 1930**
(Pl. 3, Fig. 15)
1930. *Bolivina hebes* MACKFADYEN p. 59, pl. II, figs. 5a–c
1999. *Bolivina hebes* MACKFADYEN-ABUL-NASR & SALAMA, p. 127, fig. 17 (13)
- Cassidulina laevigata* D'ORBIGNY, 1826**
(Pl. 3, Fig. 16)
- 1826 *Cassidulina laevigata* D'ORBIGNY, p. 282, pl. XV, figs. 4–5
- 1999 *Cassidulina laevigata* D'ORBIGNY-ABUL-NASR & SALAMA, p. 127, fig. 17 (20)
- Globocassidulina oblonga* (REUSS), 1850**
(Pl. 3, Fig. 17)
1850. *Cassidulina oblonga*, REUSS, p. 376, pl. 48, figs. 5–6
1982. *Globocassidulina oblonga* (REUSS)-AGIP, p. 43, fig. 7
- Bulimina elongata* D'ORBIGNY, 1826**
(Pl. 3, Fig. 18)
1826. *Bulimina elongata* D'ORBIGNY, p. 269
1990. *Bulimina elongata* D'ORBIGNY-ABU EL ENEIN, pl. 8, fig. 19
- Uvigerina cf. asperula* CZJZEK, 1848**
(Pl. 3, Fig. 19)
- 1848 *Uvigerina asperula* CZJZEK, p. 146, pl. 13, figs. 14–15
- 1965 *Uvigerina asperula* CZJZEK–SOUAYA, p. 317, pl. 2, fig. 26
- Uvigerina semiornata*, D'ORBIGNY 1840**
(Pl. 3, Fig. 20)
- 1840 *Uvigerina semiornata*, D'ORBIGNY, p. 16.
- 1999 *Uvigerina semiornata*, D'ORBIGNY-ABUL-NASR & SALAMA, p. 129, fig. 18 (9).
- Fursenkoina schreibersiana* (CZJZEK, 1848)**
(Pl. 3, Fig. 21)
- 1999 *Fursenkoina schreibersiana* (CZJZEK)-ABUL-NASR & SALAMA, p. 129, fig. 18 (2)
- Nodosarella* sp.**
(Pl. 3, Fig. 22)
- Cancris auriculus* (FICHTEL & MOLL), 1798**
(Pl. 3, Fig. 23)
1798. *Nautilus auriculus* FICHTEL & MOLL 1798, p. 108, pl. 20, figs. a–c
1985. *Cancris auriculus* (FICHTEL & MOLL 1798)-PAPP & SCHMID, p. 61, pl. 52, figs. 7–13
- Natlandia cf. secasensis* MCCULLOCH 1977**
(Pl. 3, Fig. 24)
1977. *Natlandia secasensis* MCCULLOCH, p. 346
- Valvulineria complanata* (D'ORBIGNY, 1846)**
(Pl. 3, Figs. 25–26)
1846. *Rosalina complanata* D'ORBIGNY, p. 175, pl. 10, figs. 13–15
1965. *Valvulineria complanata* (D'ORBIGNY)-SOUAYA, p. 44, pl. 1, figs. 9a–b
- Neoeponides* sp.**
(Pl. 3, Fig. 27; Pl. 4, Fig. 1)
- Cibicoides* sp.**
(Pl. 4, Fig. 2)
- Eponidella cf. libertadensis* CUSHMAN & HEDBERG, 1935**
(Pl. 4, Fig. 3)
- 1935 *Eponidella libertadensis* CUSHMAN & HEDBERG, p. 13
- Asterigerina planorbis* D'Orbigny, 1846b**
(Pl. 4, Figs. 4–5)
1846. *Asterigerina planorbis* D'Orbigny, p. 205, pl. 11, figs. 1–3
1931. *Discorbis planorbis* (D'Orbigny)-Macfadyen, p. 97, pl. 4, figs. 8a–c
1965. *Asterigerina planorbis* D'Orbigny-Souaya, p.34.
- Nonionellina labradorica* (DAWSON, 1860)**
(Pl. 4, Figs. 6–7)
1860. *Nonionina labradorica* DAWSON, p. 191
1988. *Nonionellina labradorica* (DAWSON)-LOEBLICH & TAPPAN, p. 617, pl. 689, figs. 8–17
- Melonis pompiliodes* (FICHTEL & MOLL, 1798)**
(Pl. 4, Figs. 8–9)
1798. *Natilus pompiliodes* FICHTEL & MOLL, p. 31, pl. 2, figs. a–c
1969. *Nonion pompiliodes* (FICHTEL & MOLL)-OMARA & OUDA, p.586, pl. 2, figs. 31–32

PLATE 3



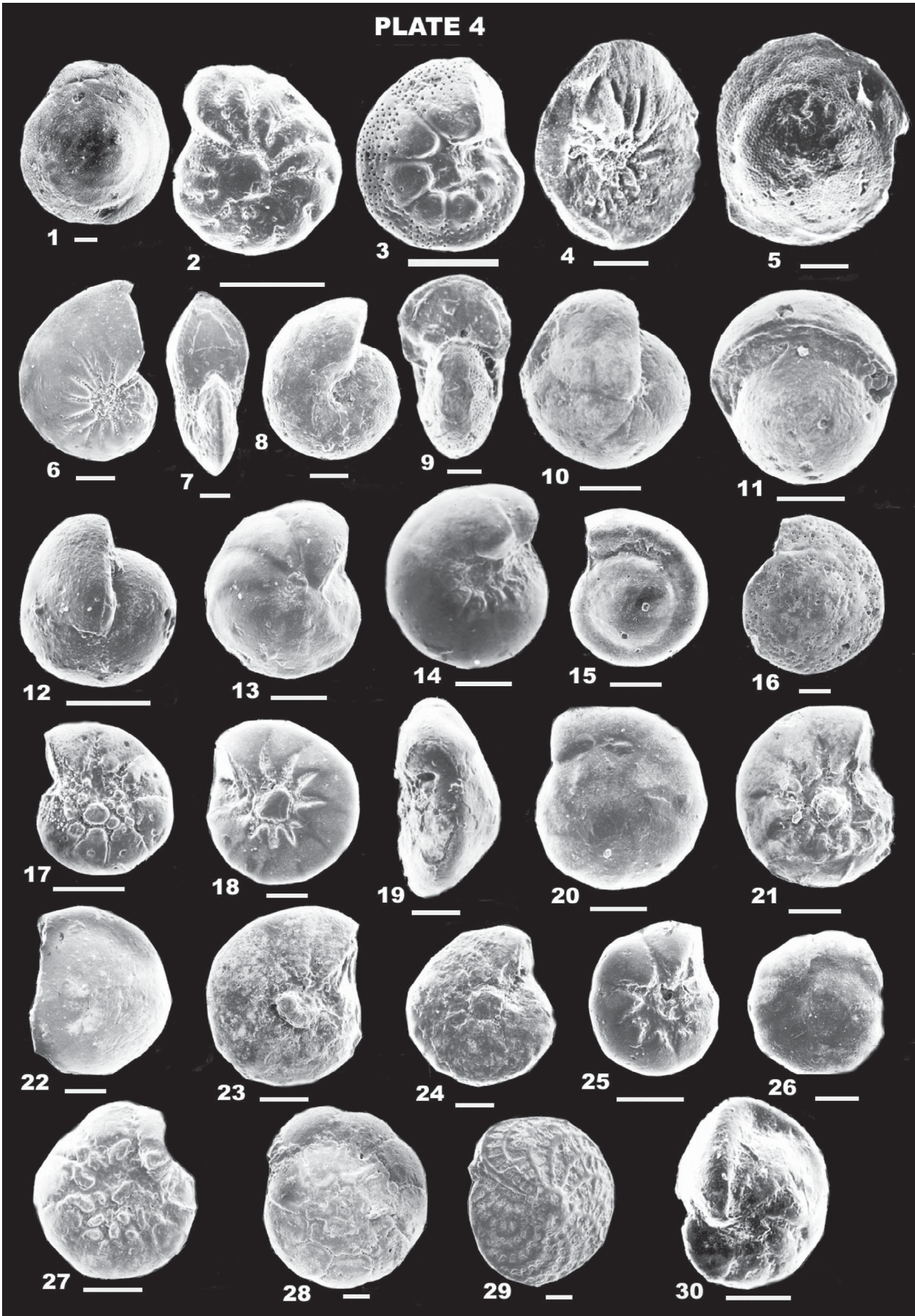
- 1999 *Melonis pompiliodes* (FICHTEL & MOLL)-ABUL-NASR & SALAMA, p. 130, fig. 19 (13–14)
- Pullenia osloensis* FEYLING & HASSAN, 1954**
(Pl. 4, Figs. 10–11)
1954. *Pullenia osloensis* FEYLING & HASSAN, p. 194, pl. 1, figs. 33–35
1983. *Pullenia osloensis* FEYLING & HASSAN-BELANGER & BERGGREN, p. 341, pl. 5, figs. 2a–3b
- Pullenia quinqueloba* (REUSS) 1851,**
(Pl. 4, Fig. 12)
1851. *Pullenia quinqueloba* REUSS, p. 71, pl. v, fig. 31
1884. *Pullenia quinqueloba* (REUSS)-BRADY, p. 617, pl. lxxxiv, figs. 14–15
- Alabamina* sp.** (Pl. 4, Fig. 13)
- Gyroidinoides soldanii* D'ORBIGNY 1825,**
(Pl. 4, Figs. 14–15)
1825. *Gyroidina soldanii* D'ORBIGNY, p. 278
1990. *Gyroidina soldanii* D'ORBIGNY-ABU EL ENEIN, pl. 12, fig. 12
- Buccella* sp.**
(Pl. 4, Fig. 16)
- Ammonia beccarii* (LINNE),**
1758 (Pl. 4, Figs. 17–20)
1758. *Nautilus beccarii* LINNE, p. 1162
1930. *Rotalia beccarii* (LINNE)-MACFADYEN, p. 103
1990. *Ammonia beccarii* (LINNE)-ABU EL ENEIN, pl. 13, fig. 4
- Ammonia ikebei* (INOUE & NAKASEKO), 1951**
(Pl. 4, Figs. 21–22)
1949. *Rotalia ikebei* INOUE & NAKASEKO, p. 10, figs. 4a–c
1980. *Ammonia ikebei* (INOUE & NAKASEKO)-BILLMAN et al., p. 88, pl. 11, fig. 16

Plate 3

Bar scale = 100 µm

- 1 *Globigerinoides trilobus immaturus*, Le Roy 1939, side view, Middle Miocene, Sidi Salim, sample from 3300 m, Naf-3 well.
- 2 *Globigerinoides trilobus sacculifer*, Brady 1877, ventral view, Late Pliocene, El Wastani, sample from 1630 m, Naf-3 well.
- 3–5 *Globigerinoides trilobus trilobus*, Reuss 1850,
 3. Ventral view, Early Miocene, Qantara, sample from 3550 m, Naf-101 well.
 4. Dorsal view, Late Pliocene, Kafr El Sheikh, sample 1960 m, Naf-2 well.
 5. Side view, Late Pliocene, Kafr El Sheikh, sample 1960 m, Naf-2 well.
- 6–8 *Sphaeroidinellopsis disjuncta*, Finlay 1940,
 6. Ventral view, Late Miocene, Rosetta, sample from 3030 m, Naf-101 well.
 7. Dorsal view, Late Miocene, Rosetta, sample from 2970 m, Naf-3 well.
 8. Side view, Late Miocene, Rosetta, sample from 2970 m, Naf-3 well.
- 9 *Orbulina bilobata*, D'Orbigny 1846, Dorsal view, Early Pliocene, Kafr El Sheikh, sample from 3075 m, Naf-2 well.
- 10 *Orbulina* cf. *suturalis* Bronnimann, 1951 Middle Miocene, Sidi Salim, sample from 3300 m, Naf-3 well.
- 11 *Orbulina universa*, D'Orbigny 1939, Middle Miocene, Sidi Salim, sample from 3300 m, Naf-3 well.
- 12–13 *Praeorbulina glomerata curva*, Blow 1956,
 12. Ventral view, Pliocene, Kafr El Sheikh, sample from 2680 m, Naf-101 well.
 13. Middle Miocene, Sidi Salim, sample from 3300 m, Naf-3 well.
- 14 *Praeorbulina glomerata glomerata*, Blow 1956, Middle Miocene, Sidi Salim, sample from 3500 m, Naf-101 well.
- 15 *Bolivina hebes* Macfadyen 1930, Late Pliocene, El Wastani, sample from 1870 m, Naf-2 well.
- 16 *Cassidulina laevigata* D'Orbigny, 1826, Pliocene, Kafr El Sheikh, sample from 1640 m, Naf-3 well.
- 17 *Globocassidulina oblonga*, (Reuss 1850), Early Miocene, Qantara, sample from 3550 m, Naf-101 well.
- 18 *Bulimina elongata* D'Orbigny 1826, Late Pliocene, El Wastani, sample from 1925 m, Naf-2 well.
- 19 *Uvigerina* cf. *asperula* Czjzek, 1848 Late Pliocene, El Wastani, sample from 1870 m, Naf-2 well.
- 20 *Uvigerina semiornata* D'Orbigny, 1840, Pliocene, Kafr El Sheikh, sample from 1790 m, Naf-3 well.
- 21 *Fursenkoina schreibersiana* (Czjzek, 1848), Pliocene, Kafr El Sheikh, sample from 1460 m, Naf-3 well.
- 22 *Nodosarella* sp., Pliocene, Kafr El Sheikh, sample from 1640 m, Naf-3 well.
- 23 *Cancriis auriculus*, (Fichtel & Moll 1798), ventral view, Pleistocene-Recent, Baltim, sample from 1550 m, Naf-3 well.
- 24 *Natlandia* cf. *secasensis* McCulloch 1977 Dorsal view, Late Pliocene, Kafr El Sheikh, sample from 1960 m, Naf-2 well
- 25–26 *Valvulineria complanata*, (D'Orbigny 1846),
 25. Dorsal view, Pleistocene-Recent, Baltim, sample from 1550 m, Naf-3 well.
 26. Ventral view, Pliocene, Kafr El Sheikh, sample from 1640 m, Naf-3 well.
- 27 *Neoeponides* sp. Ventral view, Pliocene, Kafr El Sheikh, sample from 1680m, Naf-101 well.

PLATE 4



***Ammonia perlucida* (HERON ALLAN & EARLAND), 1913**

(Pl. 4, Fig. 23–24)

1913. *Rotalia perlucida* HERON ALLAN & EARLAND, p. 139, pl. 13, figs. 7–91990. *Ammonia perlucida* (HERON ALLAN & EARLAND)-ABU EL ENEIN, pl. 13, fig. 8***Ammonia tepida* (CUSHMAN, 1926)**

(Pl. 4, Figs. 25–26)

1999 *Ammonia tepida* (CUSHMAN)-ABUL-NASR & SALAMA, p. 130, fig. 19 (29)***Ammonia umbonata* (LEROY, 1944)**

(Pl. 4, Figs. 27–28)

1944 *Rotalia umbonata* LEROY, p. 35, pl. 7, fig. 16–181980 *Ammonia umbonata* LEROY-BILLMAN et al., p. 87, pls. 6–8***Elphidium macellum* (FICHTEL & MOLL), 1798**

(Pl. 4, Fig. 29)

1798. *Nautilus macellus* FICHTEL & MOLL, p. 66, pl. 10, figs. e–k1990. *Elphidium macellum* (FICHTEL & MOLL)-ABU EL ENEIN, pl. 13, fig. 9***Nonionina scapha* (FICHTEL & MOLL, 1798)**

(Pl. 4, Fig. 30)

1798. *Nautilus scapha* FICHTEL & MOLL, p. 105, pl. XIX, figs. d–f**Plate 4**

Bar scale = 100 µm

- 1 *Neoeponides* sp. Dorsal view, Middle Miocene, Sidi Salim, sample from 3300 m, Naf-3 well.
- 2 *Cibicidoides* sp., Early Pliocene, Kafr E Sheikh, sample from 2625 m, Naf-2 well.
- 3 *Eponidella cf. libertadensis* Cushman & Hedberg, 1935 Ventral view, Pleistocene-Recent, Baltim, sample from 1550 m, Naf-3 well.
- 4–5 *Asterigerina planorbis*, D'Orbigny 1846,
4. Ventral view, Pliocene, Kafr El Sheikh, sample from 1640 m, Naf-3 well.
5. Dorsal view, Pliocene, Kafr El Sheikh, sample from 1640 m, Naf-3 well.
- 6–7 *Nonionellina labradorica* (Dawson, 1860)
6. Lateral view, Pliocene, Kafr El Sheikh, sample from 1980 m, Naf-101 well.
7. Side view, Pliocene, Kafr El Sheikh, sample from 1980 m, Naf-101 well.
- 8–9 *Melonis pompilioides*, (Fichtel & Moll 1798)
8. Lateral view, Late Pliocene, El Wastani, sample from 1540 m, Naf-101 well.
9. Side view, Late Pliocene, El Wastani, sample from 1540 m, Naf-101 well.
- 10–11 *Pullenia osloensis*, Feyling & Hassan 1954,
10. Lateral view, Late Pliocene, El Wastani, sample from 1540 m, Naf-101 well.
11. Side view, Late Pliocene, El Wastani, sample from 1540 m, Naf-101 well.
- 12 *Pullenia quinqueloba*, (Reuss 1851), Middle Miocene, Sidi Salim, sample from 3300 m, Naf-3 well.
- 13 *Alabama* sp. Ventral view, Pliocene, Kafr El Sheikh, sample from 1640 m, Naf-3 well.
- 14–15 *Gyrodinoides soldanii*, (D'Orbigny 1825),
14. Ventral view, Pliocene, Kafr El Sheikh, sample from 1680 m, Naf-101 well.
15. Side view, Pliocene, Kafr El Sheikh, sample from 1680 m, Naf-101 well.
- 16 *Buccella* sp. Dorsal view, Pliocene, Kafr El Sheikh, sample from 1640m, Naf-3 well.
- 17–20 *Ammonia beccarii*, Linne 1758,
17. Lateral view, Pleistocene-Recent, Baltim, sample from 1320 m, Naf-3 Well.
18. Ventral view, Pliocene, Kafr El Sheikh, sample from 2080 m, Naf-101 well.
19. Side view, Pliocene, Kafr El Sheikh, sample from 2080 m, Naf-101 well.
20. Dorsal view, Pliocene, Kafr El Sheikh, sample from 2080 m, Naf-101 well.
- 21–22 *Ammonia ikebei*, (Inoue & Nakaseko 1951),
21. Ventral view, Pleistocene-Recent, Baltim, sample from 1460 m, Naf-3 well.
22. Dorsal view, Pleistocene-Recent, Baltim, sample from 1460 m, Naf-3 well.
- 23–24 *Ammonia perlucida*, (Heron Allan & Earland 1913),
23. ventral view, Pleistocene-Recent, Baltim, sample from 1460 m, Naf-3 well.
24. ventral view, Pleistocene-Recent, Baltim, sample from 1460 m, Naf-3 well.
- 25–26 *Ammonia tepida*, (Cushman 1926),
25. Ventral view, Pliocene, Kafr El Sheikh, sample from 1980 m, Naf-101 well.
26. Dorsal view, Pliocene, Kafr El Sheikh, sample from 1980 m, Naf-101 well.
- 27–28 *Ammonia umbonata* (LeRoy, 1944)
27. Ventral view, Late Pliocene, El Wastani, sample from 1540 m, Naf-101 well.
28. Dorsal view, sample from 1320m, Naf-3 well, Baltim, Pleistocene-Recent.
- 29 *Elphidium macellum*, (Fichtel & Moll 1798, Pliocene, Kafr El Sheikh, sample from 1460 m, Naf-3 well.
- 30 *Nonionina scapha*, (Fichtel & Moll 1798), Early Miocene, Qantara, sample from 3530 m, Naf-101 well.

1884. *Nonionina scapha* (FICHTEL & MOLL)-BRADY, p. 730, pl. IX, fig. 14–16

1930 *Nonionina scapha* (FICHTEL & MOLL)-MACFADYEN, p. 105, pl. IV, fig. 17

6. ENVIRONMENTAL IMPLICATIONS

The environmental conditions of the Neogene rocks of the studied wells are interpreted by using the results of some palaeoecological parameters (e. g. the total number of foraminifera (T.N.F.) and planktonic/benthic ratio (P/B). The first parameter (T.N.F.) is the number of foraminiferal individuals in one gram of dry sediments. It increases with increasing water depth as mentioned by BANDY & ARNAL (1960). The planktonic/benthic ratio represents the number of planktonic foraminiferal individuals divided by the number of benthic foraminifera. It is low in near shore marine environment and increases with depth until the carbonate compensation depth (CCD) of approximately 4000 m is reached, below which only agglutinated foraminifera are found (PHLEGER, 1960). These parameters are graphically repre-

sented to reflect the vertical distribution of the foraminiferal fauna of the different rock units (Figs. 13, 14 and 15). The environmental conditions for each recognized rock unit are mentioned below based on these aforementioned parameters.

The Qantara Formation was only represented in the Naf-101 well. It underlies the Sidi Salim Formation. The facies of this formation is of non-marine clastics deposited by river currents and associated marginal marine transport processes, in a high-energy outer shelf environment. Moreover, towards the north, the environment changed to a shallow marine one where clastics and even carbonates were deposited by wave transport processes in a relatively quieter inner shelf environment. This is shown by the relatively higher values of T.N.F. and high P/B values indicating an increase in water depth as shown on Fig. 15. Also, the occurrence of *Bolivina dilatata*, *Gyroidinoides soldanii*, *Bulimina elongata* and *Globocassidulina oblonga* indicates an increase of water depth (MURRAY, 1991) as in Fig. 15.

The Sidi Salim Formation overlies the Qantara Formation and underlies the Qawasim Formation. The faunal distribution shows considered values of T.N.F., high P/B values

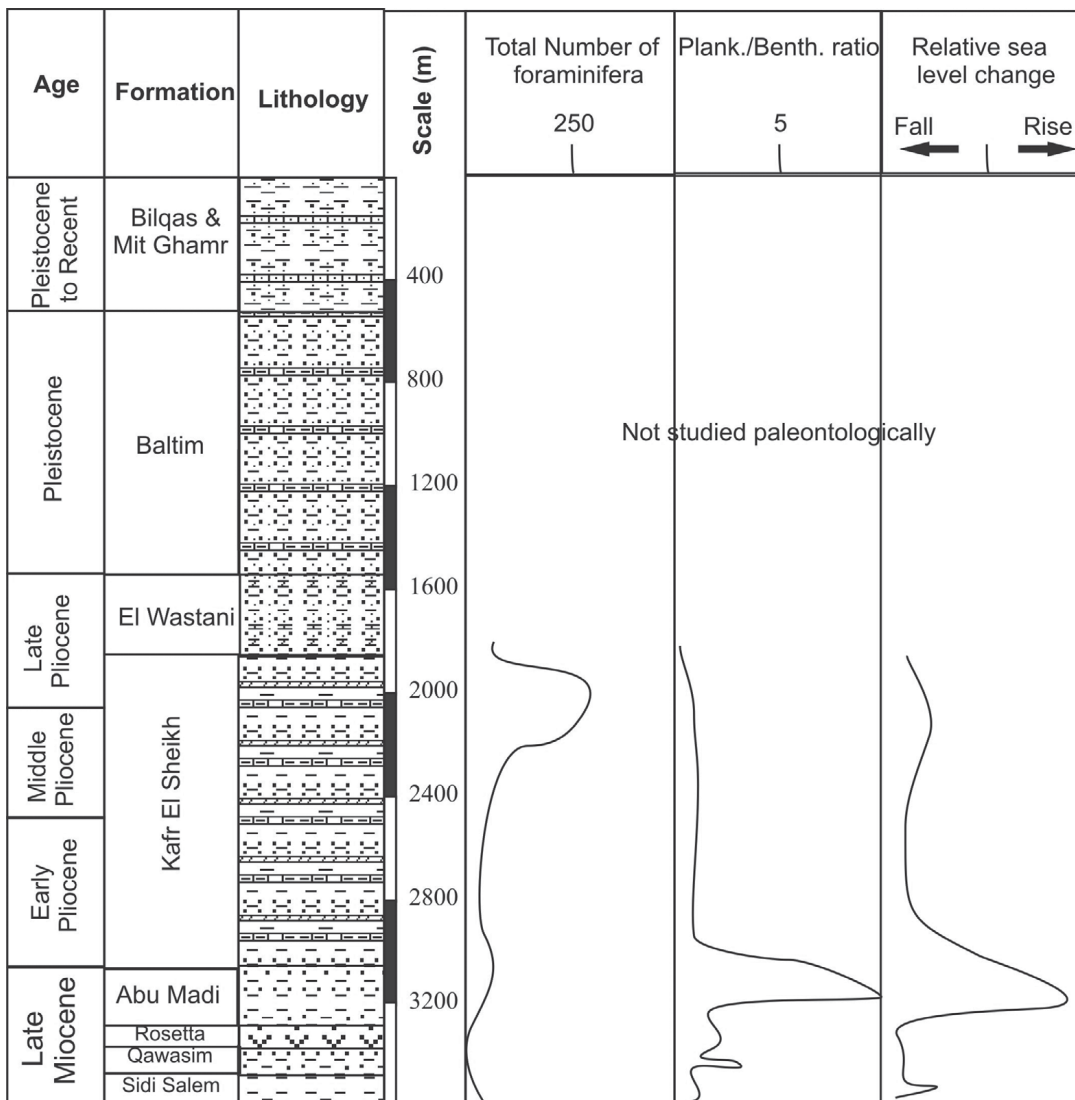


Figure 13: The paleoecological parameters of Naf-2 well.

especially in the upper part of the formation which indicate an increase in water depth. Furthermore, the occurrence of *Bolivina hebes*, *Bulimina elongata*, *Uvigerina pygmoidea*, *Gyroidinoides soldanii* and *Lenticulina antipodum* suggests a deep shelf environment (MURRAY, 1991) at the upper part of the Sidi Salem Formation. Moreover, there is a decrease in these values up to the middle of this formation as shown on Fig. 14. The facies of this formation, towards north and northwest directions, can be described as shallow marine clastics deposited primarily by wave transport processes in a relatively low-energy outer shelf environment. Furthermore, it gradually changes into a high-energy deltaic environment, towards the south and southeast, which resulted in clastic deposits being deposited from several channels.

The Qawasim Formation overlies the Sidi Salim Formation and underlies the Rosetta Formation. The values of T.N.F. and P/B ratio are relatively low indicating a decrease in water depth during deposition of this formation. It was

deposited in a high-energy deltaic environment, towards the south and southeast directions. The occurrence of *Ammonia beccarii* in the Qawasim formation in the Naf-3 well suggests a near-shore environment (VAN DER ZWAAN & JORISSEN, 1991).

The Rosetta Formation overlies the Qawasim Formation and underlies the Abu Madi Formation. This unit is extremely poor in foraminifera. It reflects a decrease in water depth during its deposition. Deposition of evaporites in this formation indicates a general regression of the whole Mediterranean. The top of this formation coincides with a general regression of sea level all over the study area, which is contemporaneous with the "Messinian Salinity Crisis" phenomenon all over the Mediterranean HSU et al. (1973, 1977).

The Abu Madi Formation overlies the Rosetta Anhydrite and underlies the Kafr El Sheikh Formation. The faunal distribution shows an increase of T.N.F. values and high P/B values indicating an increase in water depth during deposi-

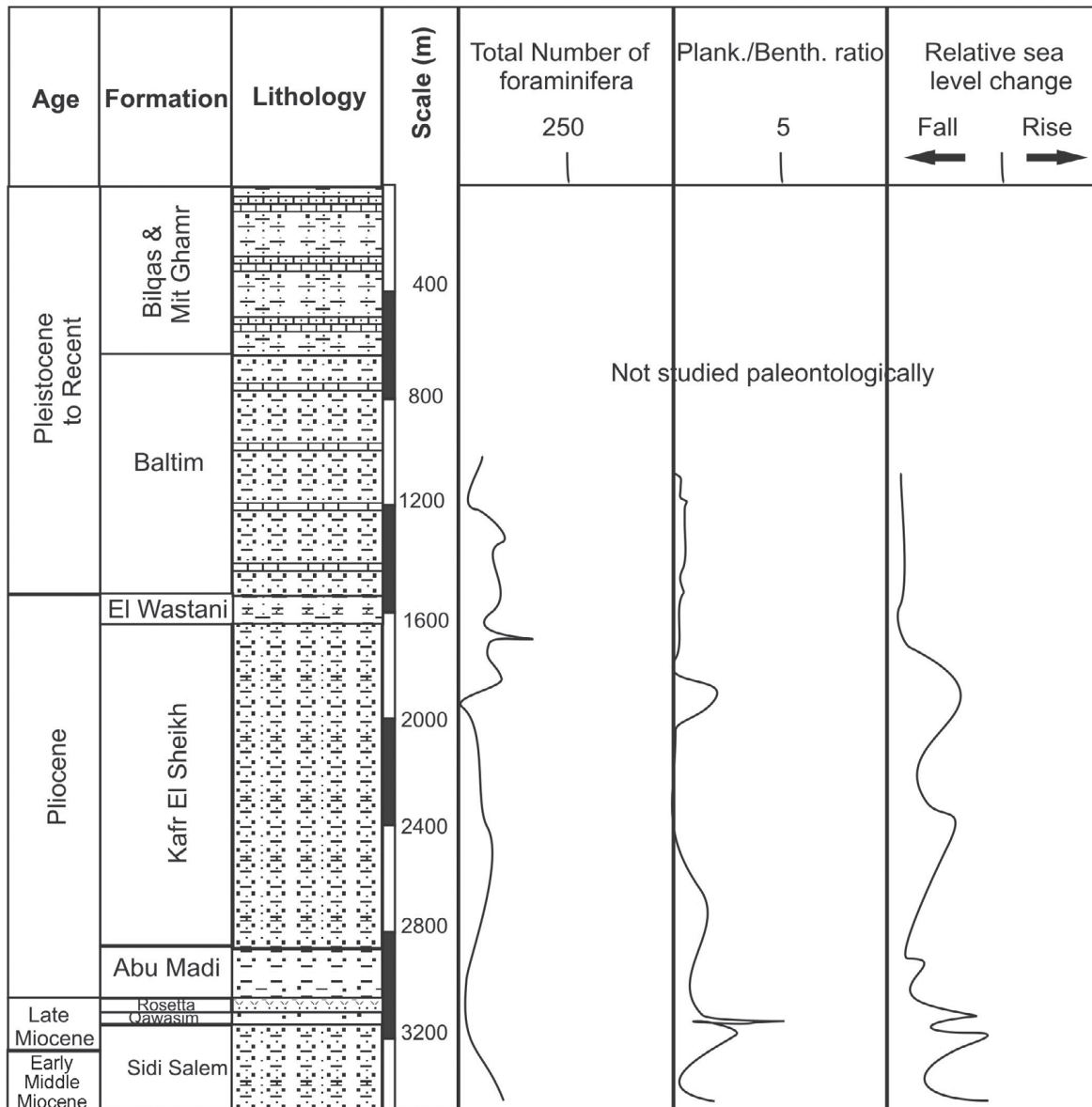


Figure 14: The paleoecologic parameters of Naf-3 well.

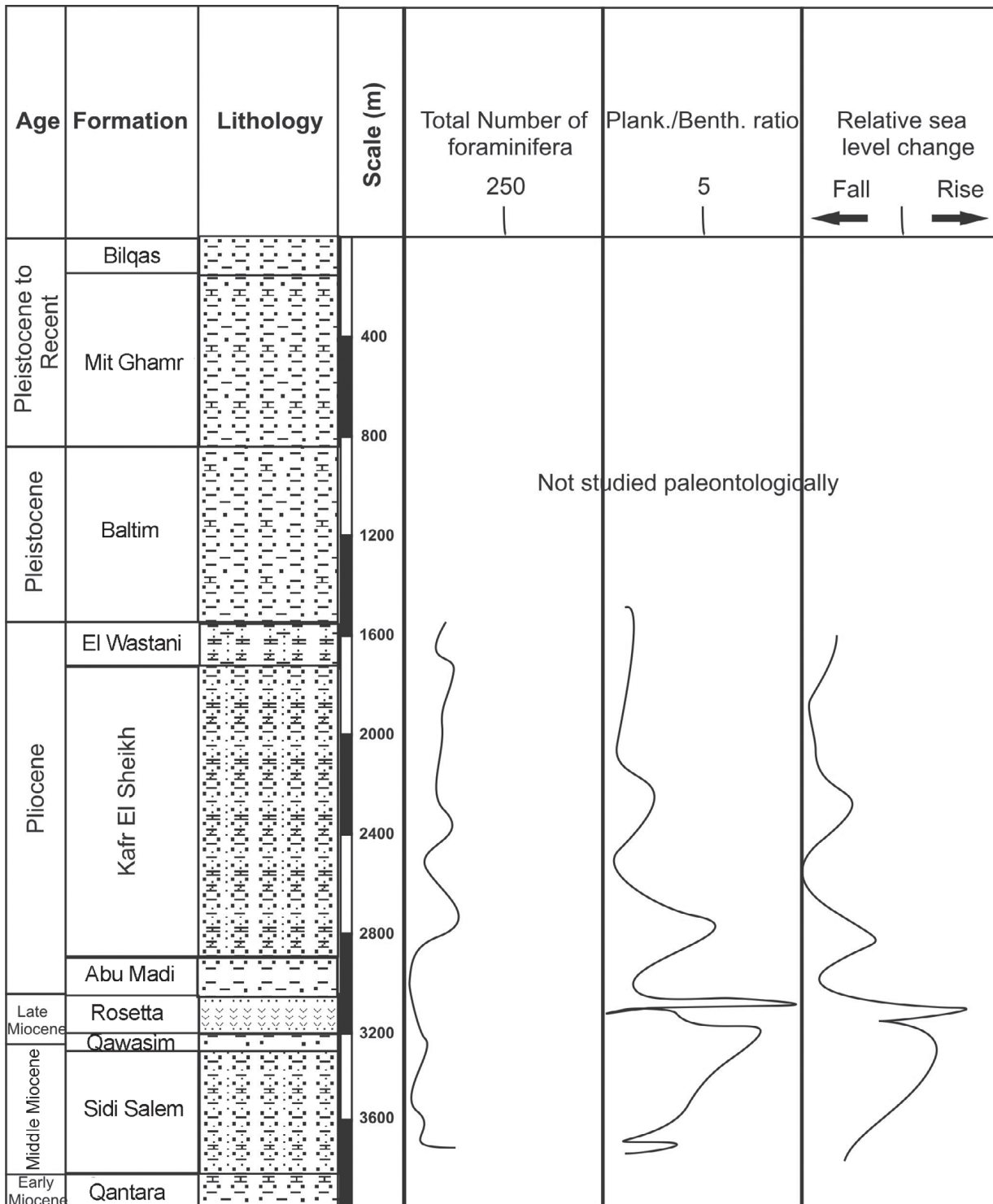


Figure 15: The paleoecologic parametres of Naf-101 well.

tion of this formation (Fig. 13). The occurrence of *Bolivina hebes* (as in Naf-3 well) reflects a neritic type of bolivines (DOUGLAS, 1979). Furthermore, the occurrence of the costate *Uvigerina semiornata* (as in the Naf-3 well) that prefers anoxic conditions and fine-grained substrate (BOERSMA, 1984) suggests a shallow environment.

The Kafr El Sheikh Formation overlies the Abu Madi Formation and underlies the El Wastani Formation. The faunal distribution reflects an increase of T.N.F. values and high

P/B values mostly at the top and the base of this formation, if compared to the middle part, indicating a fluctuating water depth which is lower for the central section of the formation. The occurrence of *Cassidulina brocha*, *Ammonia beccarii*, *A. tepida*, *Pullenia osloensis*, *Bolivina dilatata*, *Bulimina elongata*, *Uvigerina pygmoidea* and *Vulvulineria complanata* suggests a higher water depth in the lower part of the Kafr El Sheikh Formation. Also, the same conditions prevailed in the upper part of the same formation as indicated

by the occurrence of *Elphidium advenum*, *Quinqueloculina boschiana*, *Globocassidulina oblonga* and *Fursenkoina schreibersiana*.

The El Wastani Formation overlies the Kafr El Sheikh Formation and underlies the Baltim Formation. The faunal distribution of this formation reflects an increase of T.N.F. but low P/B values. This represents a lowering of the water depth during deposition of this formation as shown on Fig. 14. The top of this formation coincides with a regression of sea level all over the study area. Also, the occurrence of *Ammonia-Elphidium* and *Valvulineria-Fursenkoina* assemblages suggests a near shallow environment and a decrease in water depth through the El Wastani Formation.

The Baltim Formation overlies the El Wastani Formation and underlies the Mit Ghamr Formation. The faunal distribution of this formation is only observed for the lower part (Fig. 14) due to a lack of samples. The facies in the southern parts, of the study area, can be described as shallow marine. Intercalations of sand, shales and even carbonates were deposited, primarily by wave transport processes, in a high energetic outer shelf environment which become more quiet towards the north.

The Mit Ghamr Formation overlies the Baltim Formation and underlies the Bilqas Formation. The facies can be described as clastics and even carbonates deposited in a quiet shelf environment, where these sediments were affected by postdepositional processes forming some sort of canyon in the older sediments.

Finally, the Bilqas Formation covers the whole delta. AZZAM (1994) mentioned that during this time, the marine transgression covered most of the northern delta area and gave rise to a few metres of marine sediments capped by agricultural soil. This is repetition whereas this section is about the faunal content and depositional environment, where no samples are available in this interval.

7. CONCLUSION

The present work deals with the stratigraphy and micropaleontology of the sedimentary sequence in the North Abu Qir Field, Nile Delta, Egypt. Three wells (Naf-2, Naf-3 and Naf-101) were described, sampled and micropalaeontologically investigated. The lithostratigraphic studies have been carried out on the study area helped in the recognition of the Miocene–Pliocene rock units of the study area. These units are (from base to top) the Qantara Formation, Sidi Salim Formation, Qawasim Formation, Rosetta Formation, Abu Madi Formation, Kafr El Sheikh Formation, Baltim Formation, Mit Ghamr Formation, and Bilqas Formation.

The Qantara Formation is dated as Early Miocene according to the presence of *Globigerinoides primordius*. This age assignment is confirmed by the presence of the Early Miocene forms such as *Globoquadrina altispira altispira* and *Globorotalia obesa* (KENNETT & SRINIVASAN, 1983). The Sidi Salim Formation is of Middle Miocene age due to the presence of *Globigerinoides bollii*, at the top of this formation, which could represent a useful datum in the

Mediterranean, where the *Globorotalia fohsi* lineage is not developed (BOLLI & SAUNDERS, 1985). On the other hand, the absence of the three upper biozones of the Middle Miocene (*Globigerinoides ruber*, *Globorotalia mayeri* and *Globorotalia menardii* biozones) indicates a hiatus between the Middle and Late Miocene. However, the presence of *Praeorbulina glomerata curva* and *Praeorbulina glomerata glomerata* species supports an Early Middle Miocene age for this formation, which is directly overlain by the Upper Miocene sediments. This indicates a hiatus between the Early Middle and Late Miocene. Accordingly, this formation is dated as being from the Early Middle to Late Miocene. The Qawasim Formation is dated to the Late Miocene according to its stratigraphic position between the underlying Sidi Salim Formation of Early Middle Miocene to Late Miocene age and the overlying Rosetta Formation of Late Miocene. This Rosetta Formation is of Late Miocene (Messinian) age, due to its stratigraphic position below the well-defined Early Pliocene marine sediments, together with, the presence of the definitive *Sphaeroidinellopsis disjuncta* in the topmost part of this formation.

REFERENCES

- ABU EL ENEIN, M.A. (1990): Contribution to the Miocene stratigraphy of the Nile Delta. PH.D. Thesis, Geology Department, Faculty of Science, Ein Shams University, Cairo, Egypt, 186 p.
- AZZAM, A.S. (1994): An integrated seismo-facies and seismo-tectonic Study of the Nile Delta of Egypt, utilizing common-depth seismic reflection data. PH.D. Thesis, Geology Department, Faculty of Science, Ein Shams University, Cairo, Egypt, 240 p.
- BADRAN, A.M. (1996): The contribution of logging analysis and seismic Stratigraphy in the reservoir valuation and Lithology Determination of the north western Delta Abu Qir Offshore Egypt. MS.C. Thesis, Geophysics Department, Faculty of Science, Ein Shams University, Cairo, Egypt, 112 p.
- BARAKAT, M.G. (1982): General review of the petroliferous provinces of Egypt with special emphasis on their geological setting and oil Potentialities. Geology Department, Faculty of Science, Cairo University, Cairo, Egypt, 87 p.
- BOERSMA, A. (1984): Handbook of common Tertiary *Uvigerina*. – Microclimates Press, N.Y., 207 p.
- BOLLI, H.M. & SAUNDERS, J.B. (1985): Oligocene to Holocene low latitude Planktic Foraminifera. – In: BOLLI, H.M., SAUNDERS, J.B. & PERCH-NIELSEN, K. (eds.): Plankton Stratigraphy. Cambridge earth science series, Cambridge University Press, 155–262.
- CITA, M. B. (1975): The Miocene/Pliocene boundary: history and definition. Micropaleontology, Special Publication, 1, 1–30.
- DEIBIS, S., FUTYAN, A.R.T., INCE, D.M., MORLEY, R.J., SEYMOUR, W.P., THOMPSON, S. (1986): The stratigraphy framework of The Nile Delta and its implications with respect to the region's hydrocarbon Potential. EGPC, Eighth Exploration Conference Centenary of first oil well, Nov. 7–23, 15 p.
- DOUGLAS, R.G. (1979): Benthic foraminiferal ecology: A review of concepts and methods. – In: LIPPS, J.H. et al. (eds.): Foraminiferal paleoecology. SEPM Short Course, 6, 21–53.
- E.G.P.C. (1994): Nile Delta and North Sinai. Fields, discoveries and hydrocarbon potentials. Cairo, Egypt.
- EFFAT, A. & EL GEZEIRY, M. (1986): New aspects for Abu Qir stratigraphic and sedimentologic model. Wepco, P.O. Box 412, Alex., Egypt.

- HSU, K.J., RYAN, W.B.F. & CITA, M.B. (1973): Late Miocene desiccation of the Mediterranean.– *Nature*, 242, 240–244.
- HSU, K.J., MONTADERT, L., BERNOULLI, D., CITA, M.B., ERICKSON, A., GARRISON, R.E., KIDD, R.B., MELIERES, F., MULLER, C. & WRIGHT, R. (1977): History of the Mediterranean salinity crisis.– *Nature*, 267, 399–403.
- ISMAIL, A.A. (1984): Quantitative well logging analysis on some subsurface Successions in the Nile Delta area. MS.C. Thesis, Geology Department, Faculty of Science, Ain Shams University, Cairo, Egypt, 214 p.
- KENNETT, P. & SRINIVASAN, M.S. (1983): Neogene Planktonic Foraminifera A phylogenetic atlas. University of Rhode Island, distributed Worldwide by Van Nostrand Reinhold Company Inc., 135w. 50th Street, New York, N Y 10020, 265 p.
- MACFADYEN, W.A. (1930): Miocene foraminifera from the Clysmic area of Egypt and Sinai.– *Geol. Surv.*, Egypt, 1–149.
- MURRAY, J.W. (1991): Ecology and paleoecology of benthonic foraminifera.– Longman Scientific and technical, England, 397 p.
- RIZZINI VESSANI, F., COCOCETTA, V. & MILAD, G. (1978): Stratigraphy and Sedimentation of Neogene-Quaternary section in the Nile Delta area.– *Marine Geol.*, 27, 327–348.
- SAID, R. (1990): The Geology of Egypt, EGPC, Conco, Hurghada Inc. and Repsol Expl. S.A., 743 p.
- SAID, R. (1975): The geological evaluation of the river Nile.– In: The prehistory of the Middle East and the Levant. South Methodist Univ. press, 7–44.
- SCHLUMBERGER (1984): Well Evaluation Conference, Egypt, *Geology of Egypt*, 1, 1–64.
- SOUAYA, F.J. (1966): Miocene foraminifera of the Gulf of Suez region, U.A.R. *Micropaleontology*, January, 1966, 12/1, 34–64, pls. 1–4.
- VAN DER ZWAAN, G.J. & JORISSEN, F.J. (1991): Biofacial pattern in river-induced shelf anoxia. – In: Tayson, R.V. & Pearson, T.H., (eds.): Modern and ancient continental shelf anoxia. *Geol. Soc. Spec. Publ.*, 58, 65–82.

Manuscript received April 27, 2009

Revised manuscript accepted November 10, 2009

Available online February 28, 2010